submitted by :

Westinghouse Electric Corporation (WEC)
Electronic Systems Group (ESG)
P.O. Box 1693
Baltimore , Maryland 21203

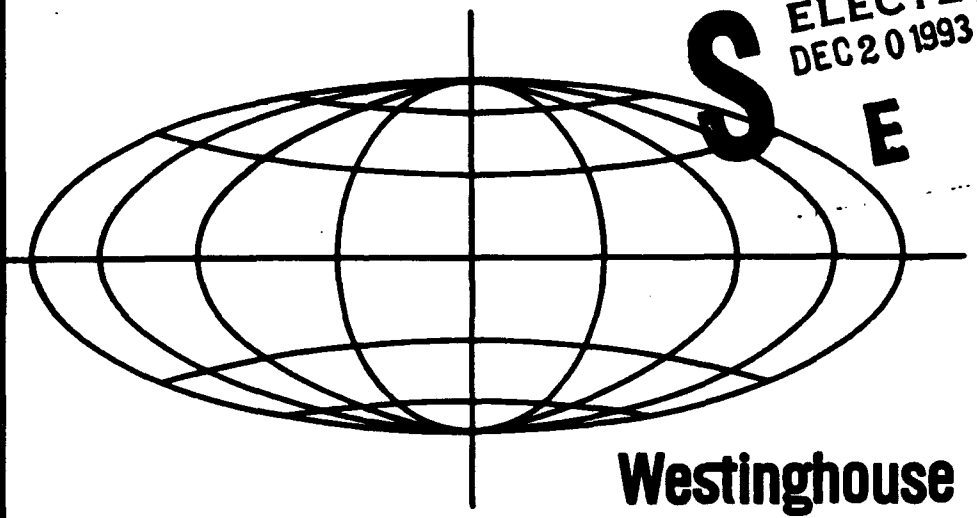

Westinghouse
ELECTRONIC SYSTEMS GROUP
BALTIMORE, MARYLAND

2

FINAL REPORT :

Meteor Burst Communications (MBC) Throughput Improvement Tests

May 1993

submitted by :

Westinghouse Electric Corporation (WEC)
Electronic Systems Group (ESG)
P.O. Box 1693
Baltimore , Maryland 21203

Sponsored by :

Defense Advanced Research Projects Agency (DARPA)
Tactical Technology Office
ARPA Order No. 7777/7

Issued by DARPA/CMO under CONTRACT# MDA DA972-91-C-0051

Table of Contents

List of Figures

List of Figures (Continued)

List of Tables

List of References

1	G.R. Sugar, "Radio Propagation By Reflection From Meteor Trails", Proceedings of the IEEE, Feb. 1964, p 130.	6
2	D.W. Brown, "A Physical Meteor-Burst Model and Some Significant Results for Communication System Design", IEEE Journal on Selected Areas in Communication, Vol. SAC-3, No. 5, September 1985	6
3	J.Z. Shanker, "Meteor Burst Communication", Artech Hourse; Boston, London, 1990, pp 89-91.	42

ABSTRACT

During the period covering October 1990 through October 1991, Westinghouse Electric Coporation (WEC) was conducting a series of WEC -internally - funded (IR &D) studies aimed at evaluating the feasibility of using meteor burst communications (MBC) on long-haul commercial trucks. These studies include an investigation four adaptive MBC beamforming techniques:

a) - the analog regenerative,
b) - the self-phasing analog,
c) - the Butler matrix and
d) - the digital adaptive.

WEC briefed DARPA on these IR&D studies and expressed a strong interest in working to develop a MBC measurements program that would satisfy mutual WEC / DARPA technical data interests in the possibility of enhancing the performance of MBC systems.

WEC was awarded a DARPA contract to conduct a series of MBC subsystems integrations tests designed to evaluate the possibility of improving the throughput performance of current MBC by roughly an order of magnitude . This means that the goal of these tests was to investigate key technologies that offered the promise of enhanceing the performance of current MBC systems such that throughput could be increased from approximately seventy-five bits per second (75 bps) to approximately 600bps. This contract award was based on then on-going WEC MBC IR&D work and the earlier MBC systems engineering experience WEC had gained as the prime contractor / systems integrator on a classified MBC network installed in the Middle East.

This report summarizes the initial work done with the analog adaptive and a high data rate non-adaptive MBC system leading to the digital adaptive processor. Performance of the digital adaptive system is given.

The contract initially requested that WEC investigate the feasibility of employing a Feedback Adaptive Variable Rate (FAVR) MBC modem integrated with Cutler, Tillotson , Kompfner (CTK) beam-forming antenna in these throughput improvement tests. Circumstances developed such that ,first the FAVR modem and then later the original CTK beam-forming antenna subsystem were not available for use during the

period of the contract ; consequently , work was largely devoted to investigations of alternate methods for implementing the functionalities of these technologies.

FINAL REPORT :
Meteor Burst Communications (MBC) Throughput Improvement Tests

1.0 EXECUTIVE SUMMARY

In October 1991 WEC was awarded a DARPA contract to test and evaluate a meteor communication analog adaptive antenna system that had been reported as being available from Broadcom Incorporated of Mawa, N.J. Detailed initial investigations of the Broadcom Incorporated analog adaptive antenna system proceeded for approximately four months ,starting in comparing, the features of an adaptive Butler matrix, the Broadcom retrodirective adaptive beam former and the digital adaptive beam former. During this period, the interest of DARPA in high throughput increased from 600 bits / seconds (b/s), initially, to several thousand b/s. Reasoning for this situation is as follows. The statement of work (MDA972-91-C-0051) calls for "an order of magnitude improvement over MIL-STD-188-135." Initially this was interpreted as 600 b/s throughput. Later as outside interest in high throughput increased, a factor of four was added to account for seasonal variations in throughput and then a factor of three to account for possible variations in the SAIC model. This led to 7200 b/sec as an ideal objective.

As a result of the time required to complete the initial investigations of the Broadcom analog adaptive system and the long lead time of certain key parts,WEC with Broadcom's concurrence, realized , in late January 1992 , that Broadcom could **NOT** gurantee that they could produce their analog adaptive antenna system in time to be used in measurements tests and demonstrations scheduled at that time for July 1992. As a result DARPA chose to make the high throughput measurements using an approach suggested by WEC which couples an analog adaptive MBC receiver and a digital adaptive MBC beam former to achieve the technical functionalities of the CTK algorithm. WEC's own internal MBC development plans had already established a set of milestones which included such a set of tests scheduled for some time after August 1992.

This report is a collection of the work leading to this decision as well as a presentation of the design of the analog adaptive antenna subsystem which coupled with the digital adaptive beam forming subsystem implements the functionality of the CTK algorithm. The digital beam forming system is also briefly described.

The digital beam forming subsystem was entirely developed and modified for the required MBC throughput improvement measurements and demonstration using WEC

internal supplied funding. WEC was motivated to provide this funding because of WEC's interest in applying MBC to the commercial trucking tracking and communications problems.

The report starts in section 2.0 by presenting the motivation for employing adaptive beamforming techniques/methods to achieve higher throughput in meteor burst communications subsystems. Then section 3.0 presents a description a description of the particular implementation of the CTK algorithm developed by Broadcom Incorporated of Mawah , New Jersey. At the outset of this project , the plan was to try to use this configuration for the intial integration tests. Section 4.0 presents a Non-Adaptive MBC system design developed by WEC that was intended to be used as contingency method for demonstrating higher throughput rates could be achieved via convential MBC equipments. This designed was later signficantly modified by SAIC's Dr. Robert Desourdis and his technical supporters. Section 5.0 presents a relatively brief description of the Digital Adaptive Beamforming processor subsystem developed by WEC , under WEC funding. WEC plans to loan DARPA the use of a personal computer (PC) based version of this subsystem to be used in MBC tests planned for late 1993 or early 1994. Section 6.0 presents a detailed description of the analog adaptive receiver developed by WEC , under the contract funds.

2.0 Adaptive Beamforming With Meteor Communication

The necessity for employing adaptive processing and beamforming methods for meteor communication is developed in Figs.1 through 4. Fig.1 shows the region of high meteor activity on a 1000 Km and a 200 Km path. These are plan views of the great circle paths between two typical terminals viewed from high above the earth. The meteor reflections occur at random in a layer of thin air about 100 Km above the earth in a region on both sides of the great circle. For the longer 1000 Km path the activity is confined to relatively small angles to the left and right, but for the short path the azimuth angle to a given meteor trail may be ±90 deg or more. The boundary of 50 % of the activity is shown. Covering these active regions with an antenna pattern limits the gain available in a nonadaptive system. For example, Fig.2 shows that the activity is covered at 1000 Km with a high gain seven element Yagi, but the activity on the 200 Km path need be covered by a low gain dipole and reflector modified to place considerable power at ±90 deg in azimuth. To increase throughput and reduce waiting time it is necessary to increase antenna gain by using these same antennas as elements in an array antenna that is directed adaptively to the meteor trail as in Fig.3. Here a typical 4 element array is used to increase the antenna gain about 6 dB, placing the now narrowed beam on the trail within the region of high activity. The same situation applies in the elevation plane. Fig.4 shows a typical side view of the 1000 Km and the 200 Km paths with meteor reflection occurring 100 Km overhead. This demonstrates the desirability of redirecting the beam adaptively in elevation as well if the antennas are also arrayed in elevation. Thus the beam should be adaptive in two space coordinates.

1. G.R.Sugar, "Radio Propagation By Reflection From Meteor Trails", Proceedings of the IEEE, Feb.1964, p 130.

2. D.W.Brown, "A Physical Meteor-Burst Model and Some Significant Results for Communication System Design", IEEE Journal on Selected Areas in Communication, Vol.SAC-3, No. 5, September 1985

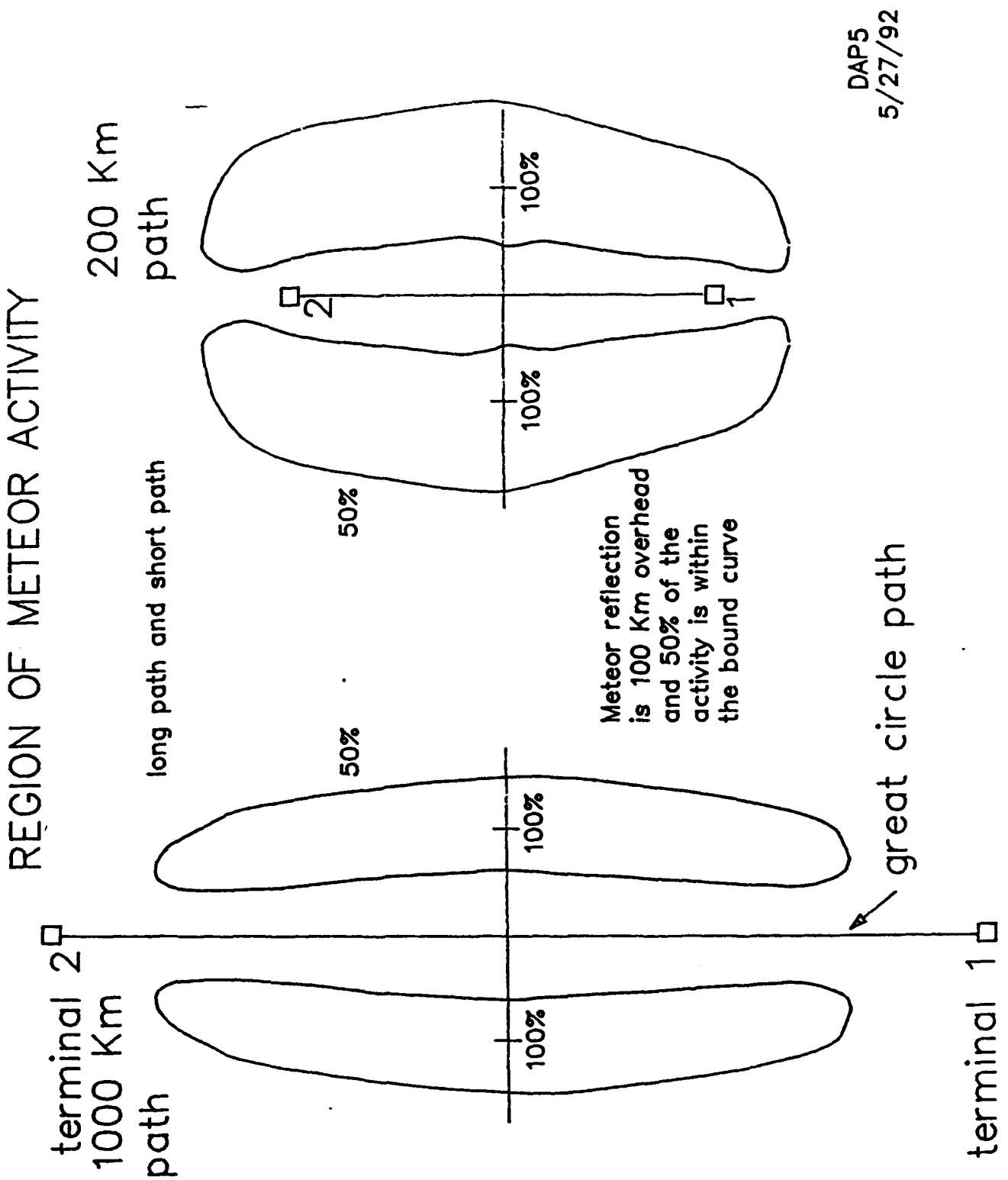

Figure 1 Region of Meteor Activity

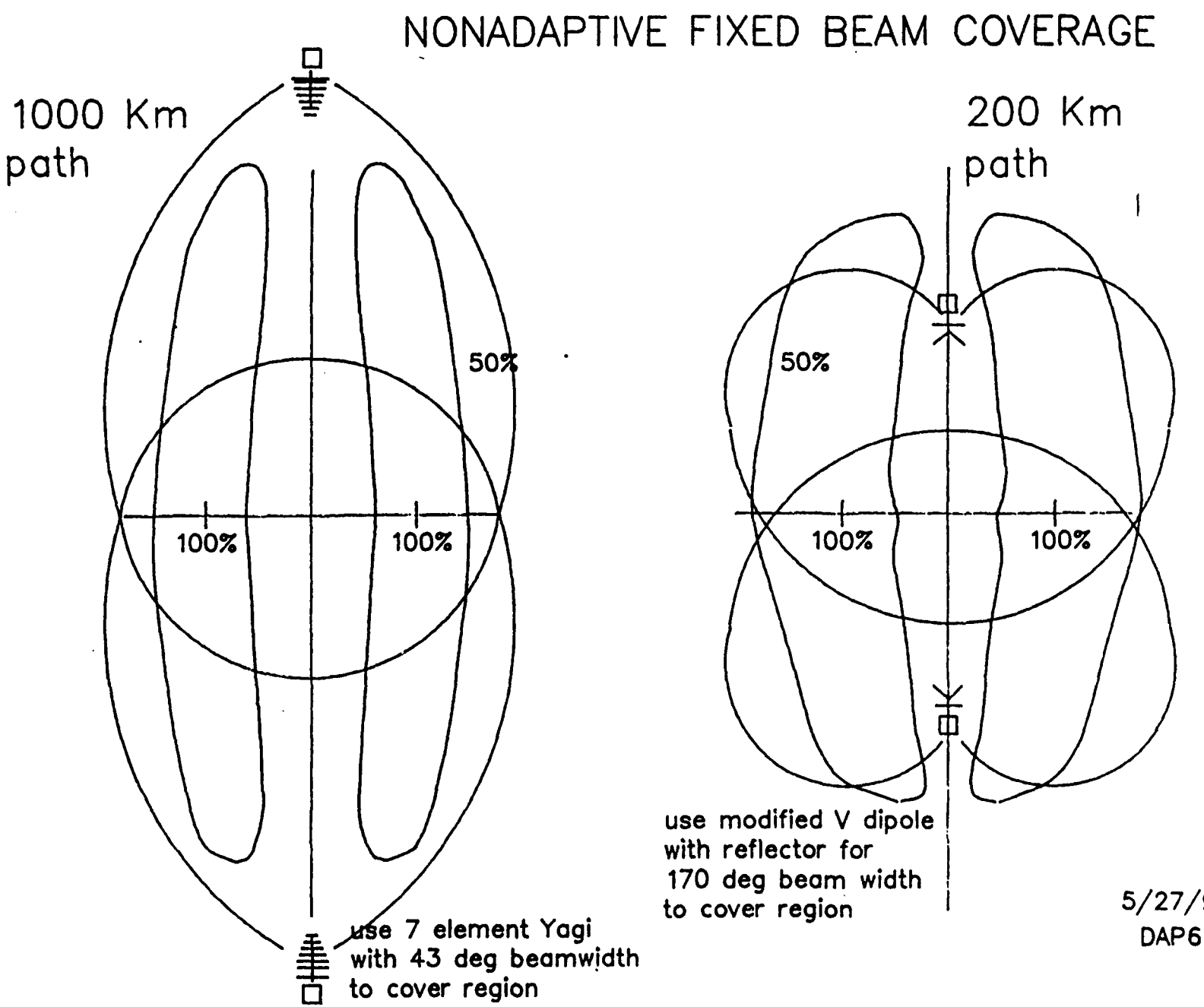

Figure 2 Nonadaptive Fixed Beam Coverage

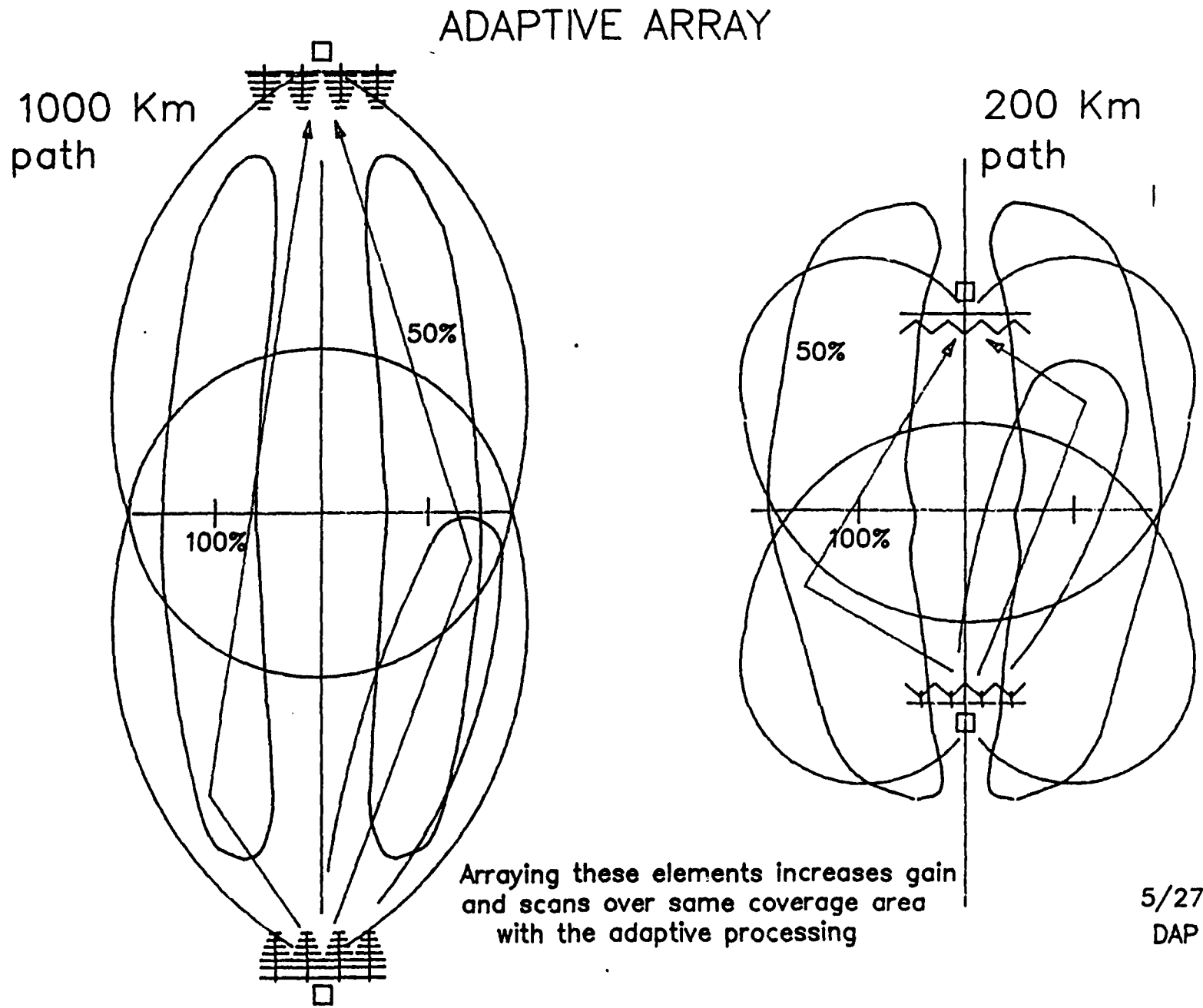

Figure 3 Adaptive Array

3.0 The Broadcom Adaptive Array

The Broadcom receive terminal was planned to have a 10 element array of four element Yagi antennas as in Fig.5. Reception was to be from a remote transmitter in a broadcast mode. The meteor trail was located by probing from the receiver with a cw tone of 300 W at 43.4 MHz (Fig.5). The retrodirective return modulated signal from the transmitter at 42.00 MHz as well another 42.50 MHz cw tone was diplexed at the receiver following the antenna. The tone was converted to 6 MHz where it was filtered with a 300 Hz bandpass crystal filter and used to selfphase the antenna array for the modulated carrier. Thus the antenna phase progression for each of the two received signals are almost identical, as they come from the same source and the carriers are so closely spaced. The phase progression from the tone is used to remove the phase progression from the desired signal. By this means an analog adaptive beam has been formed in azimuth in the direction of the transmitter. Fig.6 represents the Broadcom retrodirective transmitter. The 43.4 MHz probe is down converted to 6.0 MHz and filtered with a 300 Hz bandwidth to be used as the source for the 42.0 MHz, 300 W per antenna transmitter. Two, four element Yagi antennas are used as radiators in this array. The 42.5 MHz tone transmitter for selfphasing the receiver as explained above is also shown at 100 W. Performance is predicted in Fig.7 for the Broadcom system using the BLINK scaling model, which agrees fairly well with the complete SIAC meteor model at least in simple standard situations. It is shown meeting the 600 b/s throughput for a 9600 b/s data rate for an average month and an average time of day at a distance of 1200 Km. By the time this system was finalized, DARPA's interest in throughput had advanced to 7200 b/s even for average transmission periods. At this time SAIC showed that this kind of throughput could be attained at least at a distance of 1000 Km with a relatively large array of Yagi antennas even if used nonadaptively with certain provisions for mechanical steering. As this approach could be achieved by July it was decided to go in this direction.

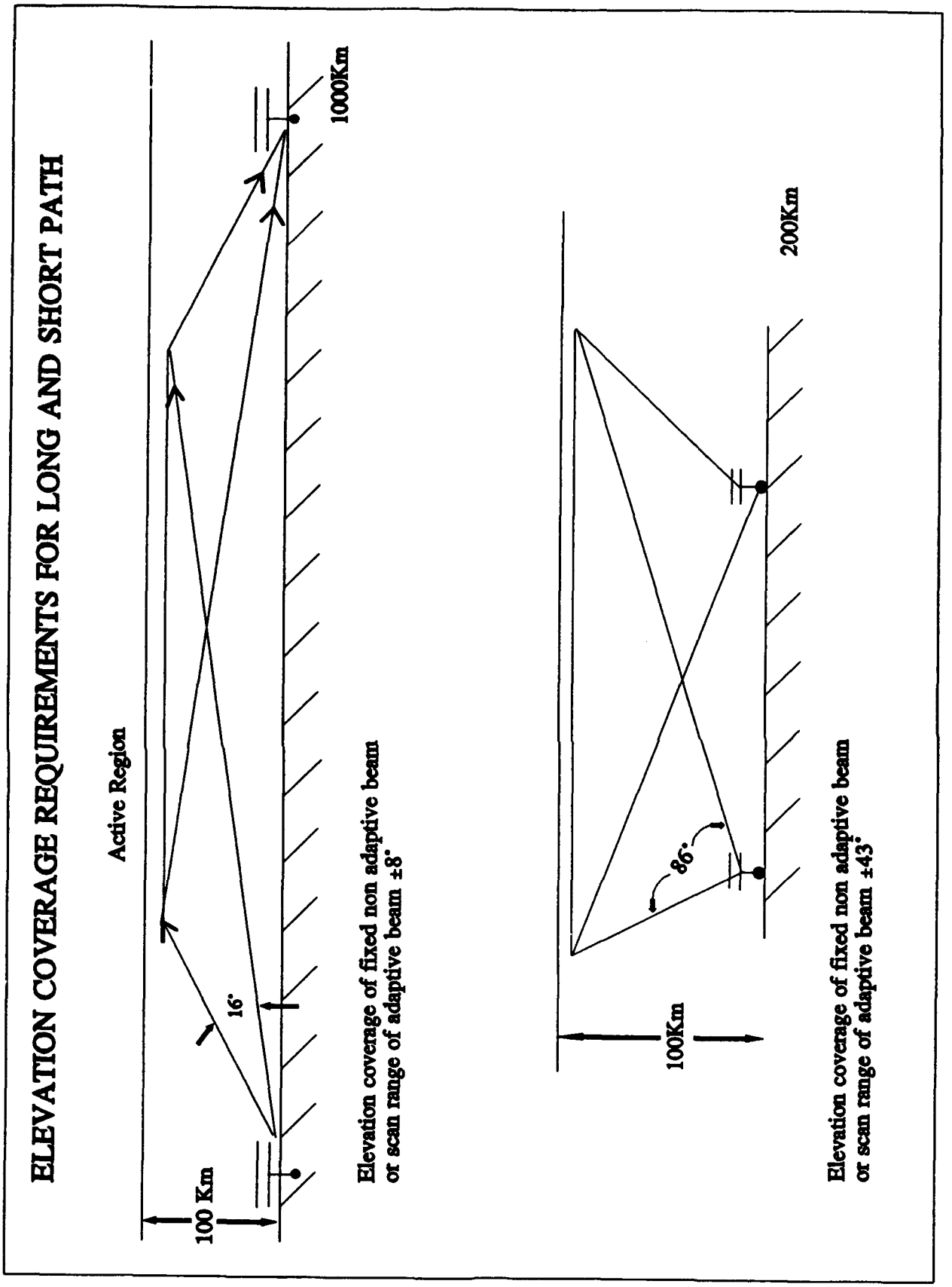

Figure 4 Elevation Coverage Requirements for Long and Short Path

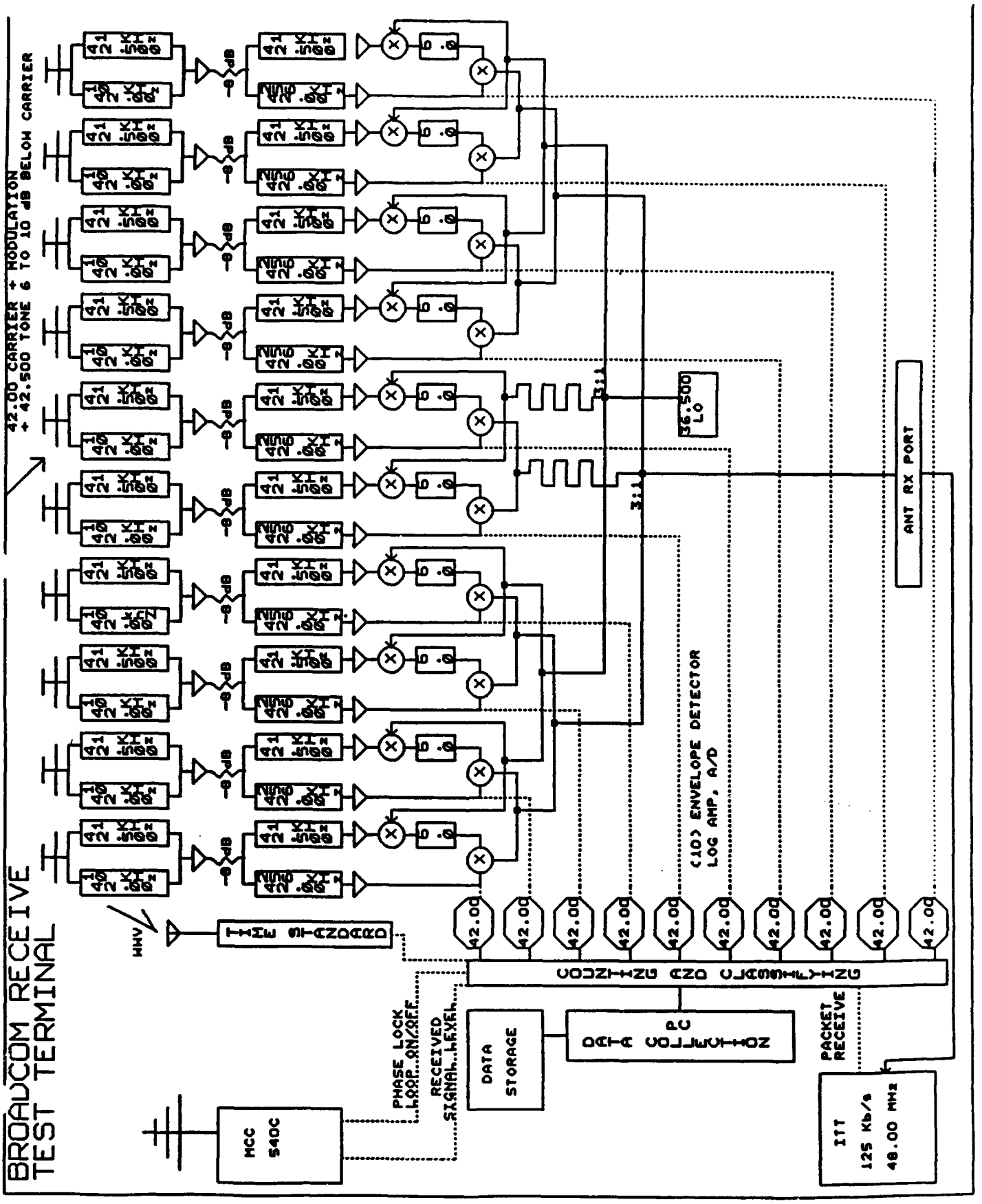

Figure 5 Broadcom Receive Test Terminal

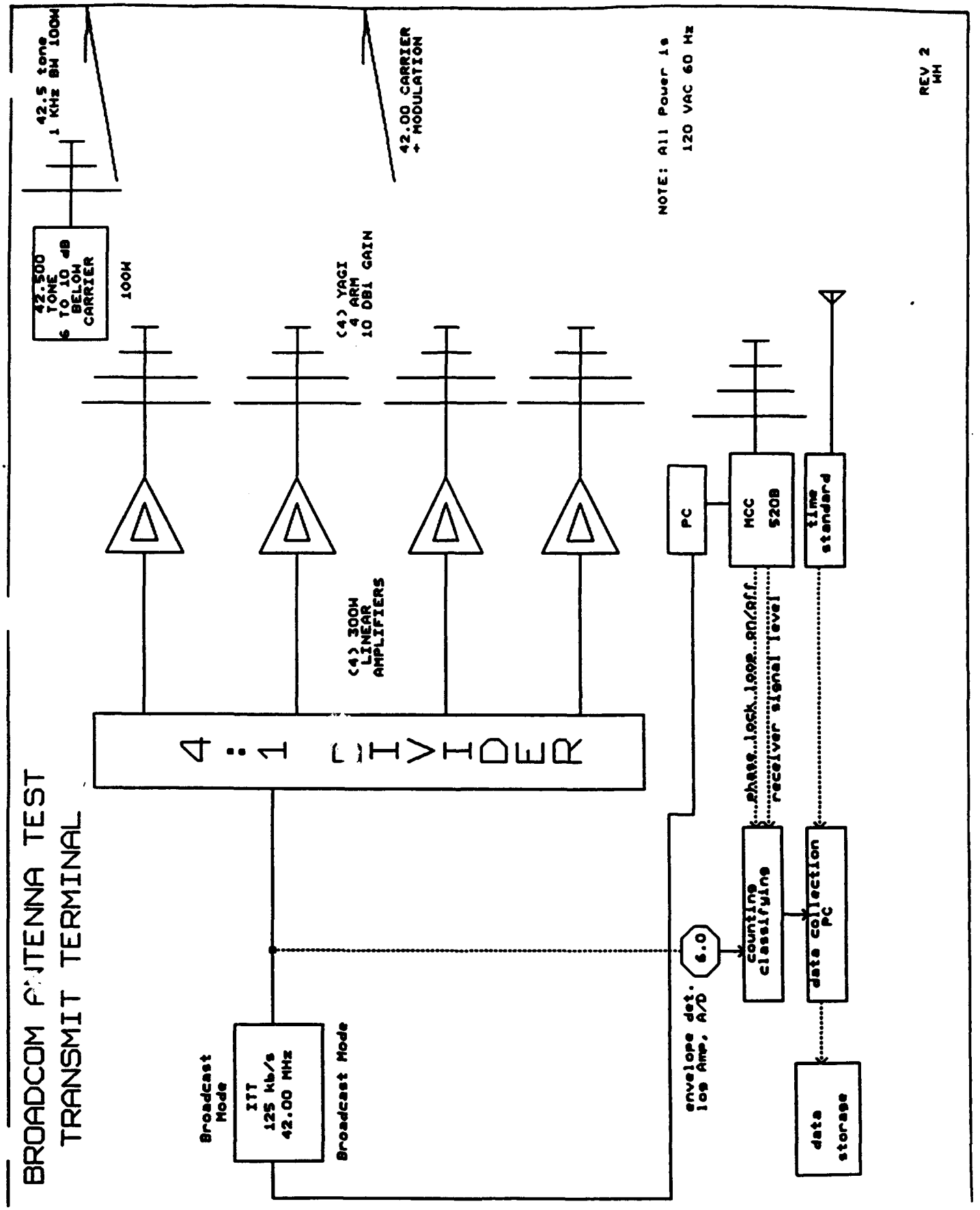

Figure 6 Broadcom Antenna Test Transmit Terminal

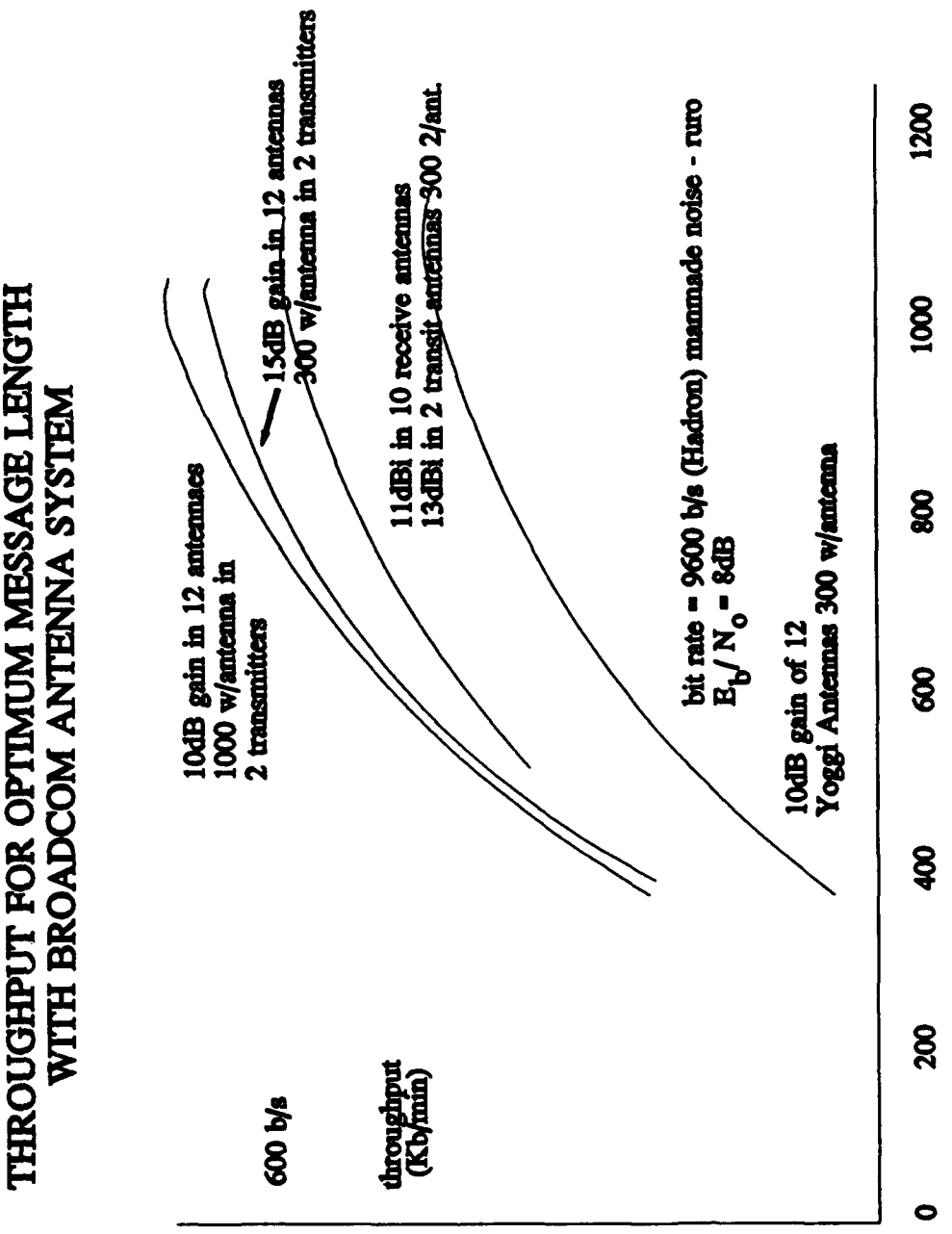

Figure 7 Throughput for Optimum Message Length
With Broadcom Antenna System

4.0 The WEC Designed Nonadaptive High Data Rate System

This section presents the engineering logic that drove the original WEC designed non-adaptive high date rate system. A 935 Km path was chosen from Cherry Point, N.C. to Rome N.Y. This is close to North/South, where during the day most of the activity is in the West sector as in Fig.8. Thus a 4 element azimuth by 2 element elevation array of (7) element Yagi antennas was modeled by SAIC and shown to have the required throughput with the 11 deg beam steered to the West of the path. The receive beam would similarly be steered to the West and they would overlap in the region of high activity for that particular time of day. Steering was to be accomplished by phase shifters in the array manifold. A phase progression is calculated on Fig.8 for this beam position of 70.4 deg per element for 1.25 wavelength element spacing. This is applied at both terminals and provides static beam positions overlapping in the meteor active region but, of course, nonadaptively.

It was realized that this was a brute force way of meeting the high throughput, but it could be achieved within the them desirable July 1992 time schedule. Fig.9 shows a block diagram of the final nonadaptive system logic with 1.2 KW for each stack of two Yagi antennas. The components list, manufacturer and cost are identified in Table I. For antennas, each end of the system has 8, (7) element Yagi antennas in a 2X4 array. The stack of two Yagis on a mast is one element of four in an azimuth array to provide a static azimuth scan as set by the azimuth phase shifters. To measure the phase shift from element to element as set by the rotary phase shifters, directional couplers are shown in Fig.9 as connecting ports for a vector voltmeter. The two elements in elevation are scanned about 5 deg above the horizon as determined by the divider network and the positioning of the antennas relative to ground. The elevation scan is not adjustable. At this time in the program a new experimental ITT modem became available operating at 125 Kb/s data rate and higher as shown in Fig.9. This high data rate made it possible to predict the 7200 b/sec throughput for the demonstration, at least in a broadcast mode of transmission. An identical system in the lower half of Fig.9 for the opposite direction of transmission was to be assembled if time and money made its use possible. Preamplifiers at each element overcome the loss in the phase shifter and cabling to the modem.

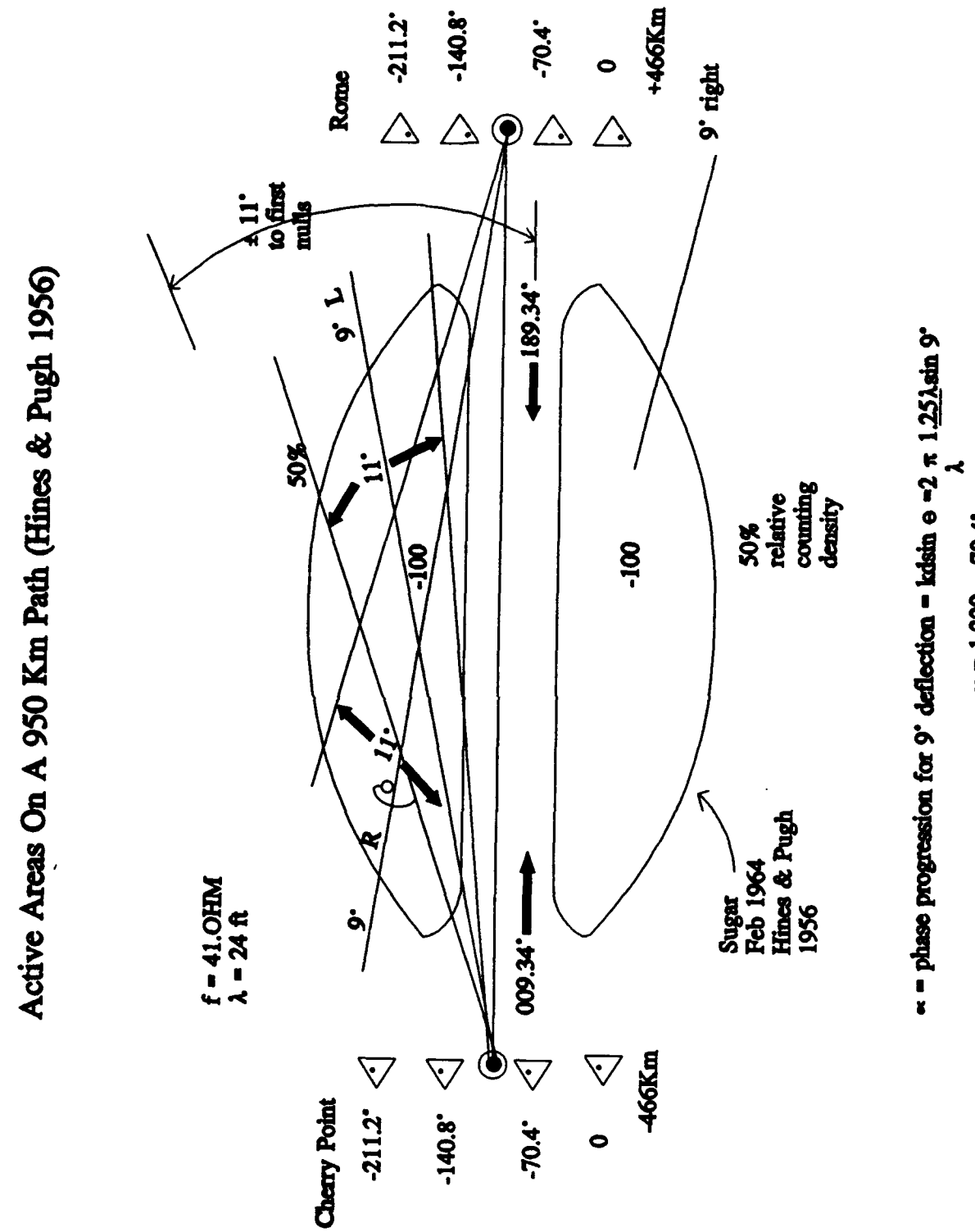

Figure 8 Active Areas On A 950 Km Path (Hines & Pugh 1956)

TABLE 1.0

The following items were planned as in Fig.9 to provide the high power-aperture product for the July 1992 nonadaptive part of the high data rate DARPA MBC test. Nominal delivery for the components was eight weeks. This list is for a single transmit receive system which is the upper half of Fig.9.

Item	Supplier	$Cost	Notes
(7)element Yagi Antenna	M2 Enterprises Fresno, California 209 432-8873 Michael Staal	16X450	30 ft. boom is short of max.gain to favor 10 ° scan
High Power Amplifier 41.00MHz, 1.2 KW linear amplifier	CreativeElectronics Arleta, California 818 897-0525 Charles Osomoto	4X5450	Includes swr cutoff harmonic filter, 20 mW drive power, type N connectors
Divider Network Consider a test of array and divider in Fresno	M2 Enterprises	2X882	Phase shifter in a matchedline section
Towers From M2 to insure compatibility with antennas	M2 Enterprises	8X910	(2) 5/8"X4X4 Marine plywood base or concrete.
Filter	Cir-Q-Tel	4X380	1 MHz bandwidth Three sections.
High Power Coupler	Werlatone N.Y. 914 279-6187 Dave Crane	4X500	For amplifier and scan calibration. Type N connectors

TABLE 1.0 (continued)

Item	Supplier	Cost	Note
10 dB Low Power Coupler DCG 104	Anzac Burlington, Vt. 617 273-3333	4X85	For scan calibration
Phase Shifter 41.0 MHz	Merrimac West Caldwell,N.J.	8X850	
Low Noise Amplifier QB 258LH-N	Q-Bit Palm Bay, Fla.	4X600	With power supply Type N connector
		---	
		$51,100	
Test Equipment			
Vector voltmeter 40-50 MHz	Hewlet Packard 8508A		relative phase and amplitude
Signal generator 40-50 MHz	Hewlet Packard 8640B		square wave and cw
Spectrum analyzer 40-50 MHz	Hewlet Packard 8592B		
adapters			

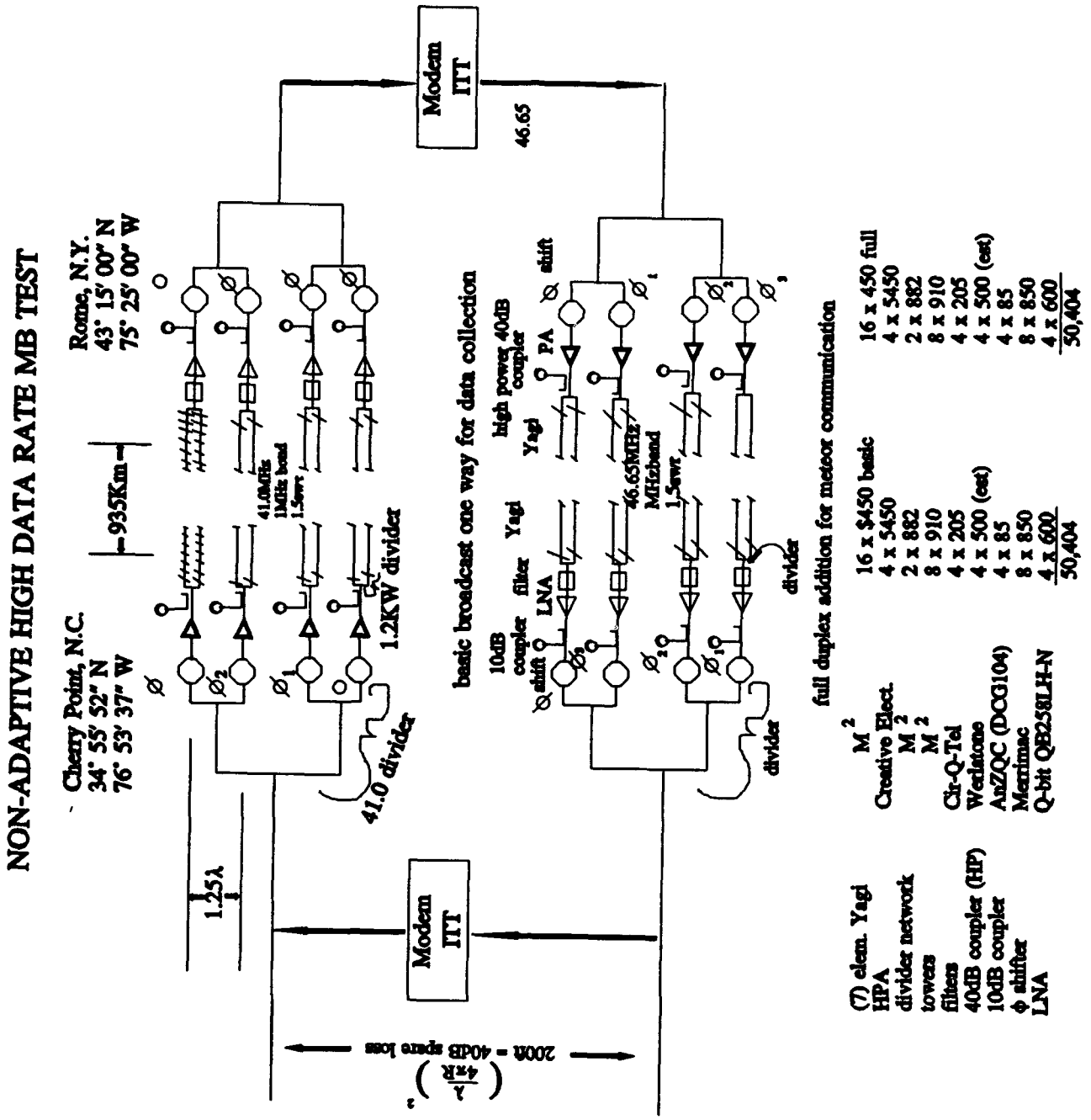

Figure 9 Non-Adaptive High Data Rate MB Test

4.1 Scanning the Yagi Arrays

The question occurs about the optimum spacing of these antennas when they are to be scanned in this fashion. This is important here in a static scan of the nonadaptive array, but the same question is important to the design of the adaptive arrays in Section II of this report. The more normal small elements in an array antenna would be spaced near 0.5 wavelengths. Such an element has a gain of _ and a receiving cross section calculated to be 0.5 wavelengths on a side as in Fig.10. With a half wave spacing the cross sections do not overlap and mutual coupling is not a big factor. For the 7 element Yagi, on the other hand, with a gain of 12.8 dBi, the receive cross section is calculated to be 1.25 wavelengths on a side (Fig.10). Thus, this is the order of spacing to be expected in order to control mutual coupling. Such an array has high gain in the unscanned position but does not scan very far with out significant loss of gain. The extent of this effect will now be evaluated. Patterns of this Yagi array element are shown in Fig.11. The upper half of 11 is the actual element pattern taken from Fig.10 as well as the assumed element pattern used to generate the three unscanned array patterns that follow for the 4X2 array. Fig.12 and 13 show the unscanned array pattern for Yagi spacings of 0.9, 1.0 and 1.25 wavelengths. As the element spacing is increased the gain increases and the side lobes increase. The side lobe increase is not important at zero scan but as scan increases the sidelobes become large enough to reduce gain. From this information as well as from similar patterns in the scanned position, a graph may be made showing the loss of gain with scan for several Yagi antenna lengths. It is shown in Fig. 14 that the 7 element Yagi can scan the required 11 deg with out significant loss of gain. It is also obvious that these elements would not be suitable on a shorter range path where, for example, a 20 deg scan is necessary. This point is sometimes overlooked in arraying these endfire elements in adaptive antennas.

RECEIVE CROSS SECTION AREA OF DIPOLE AND YAGI

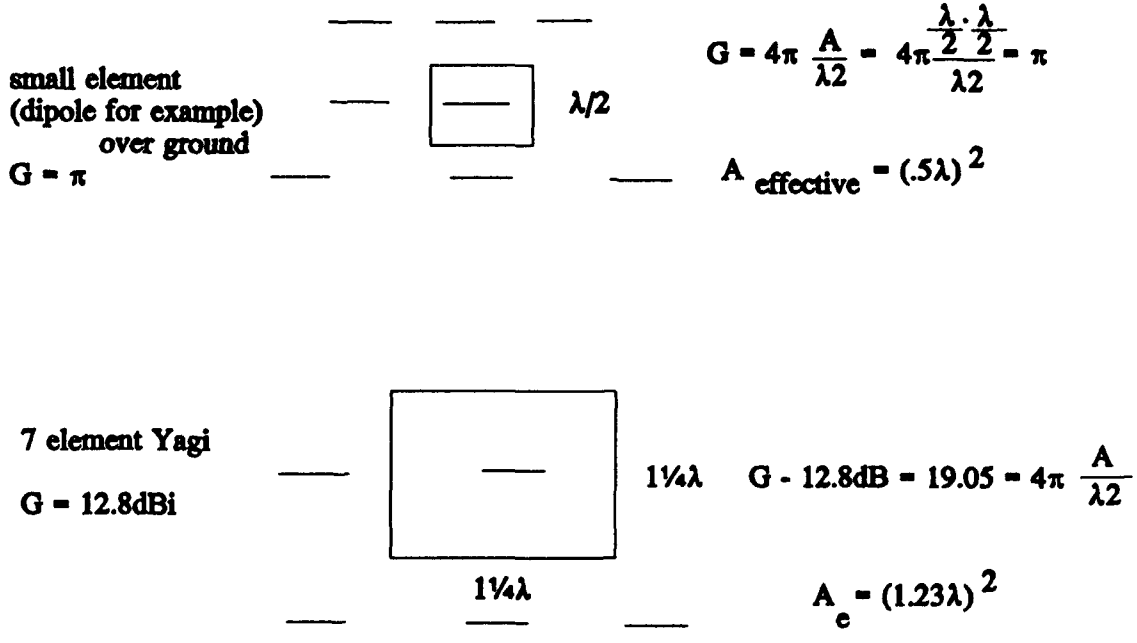

Figure 10 Receive Cross Section Area of Dipole and Yagi

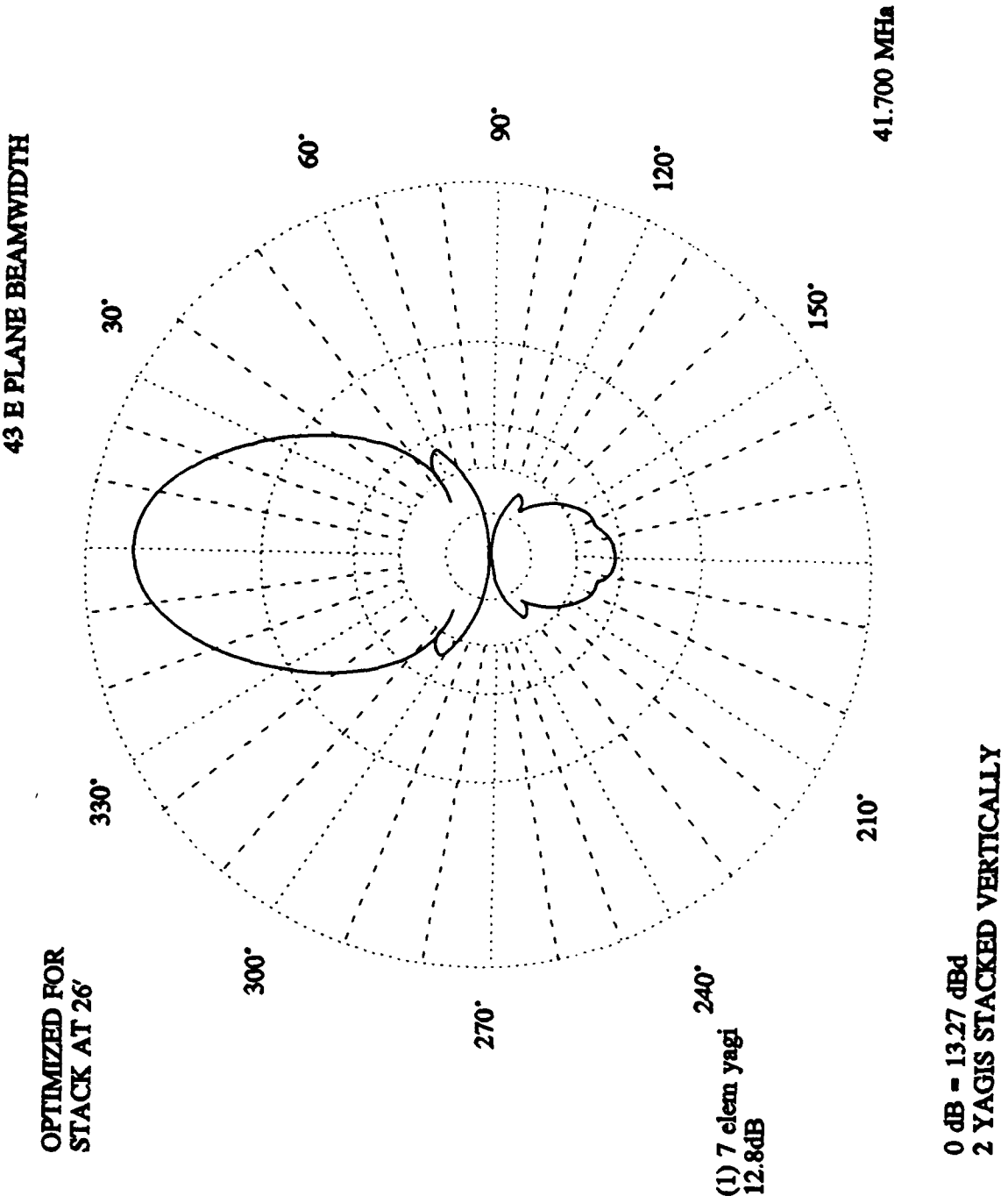

Figure 11 43 E Plane Beamwidth

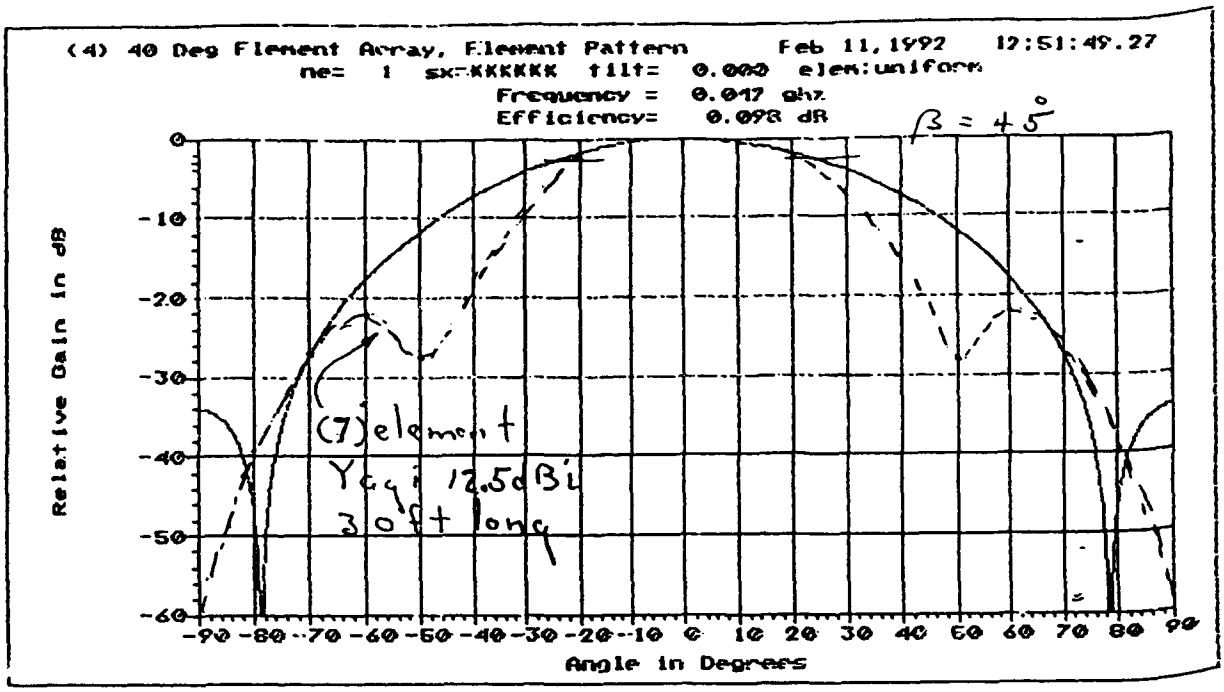

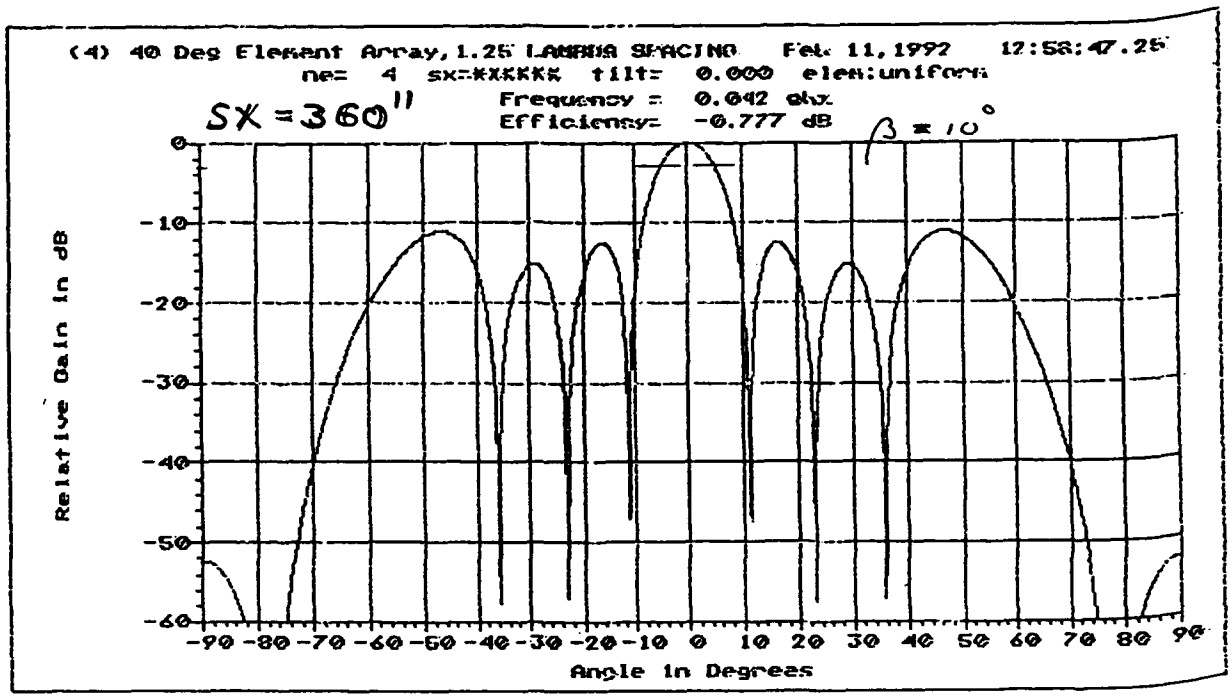

M² calls this gain 20dBi accounting for 30ft limit on Yagi length and line losses.

array 90' long

Figure 12 Array Element Patterns

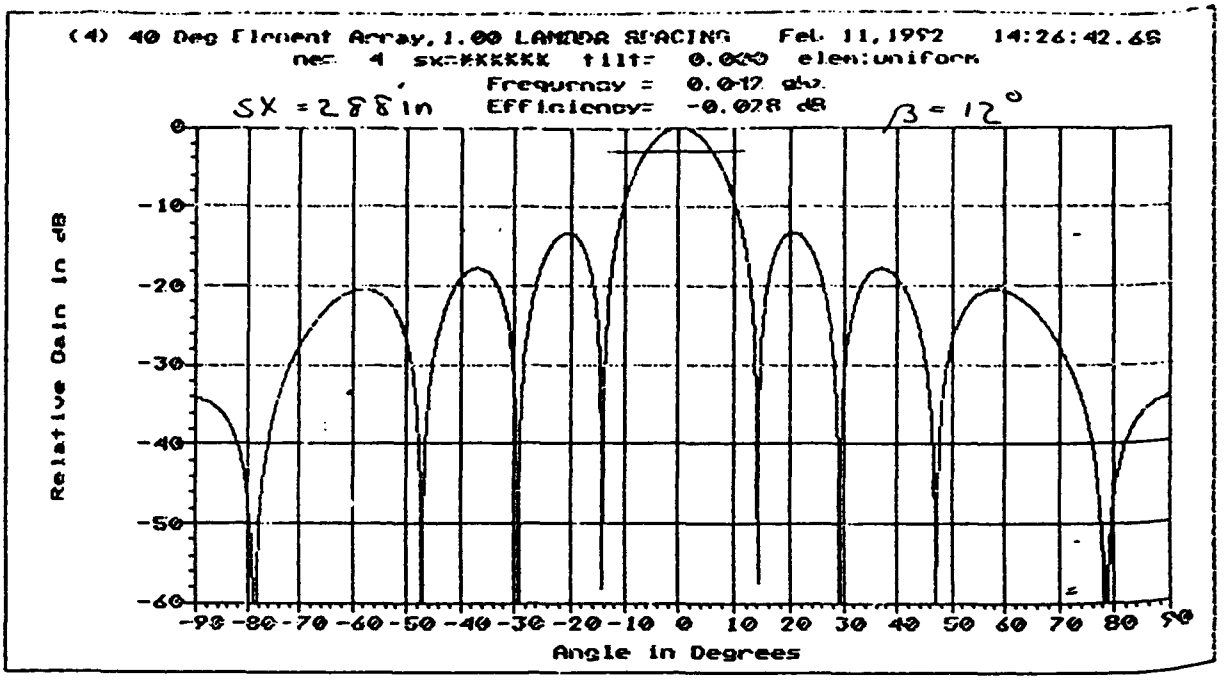

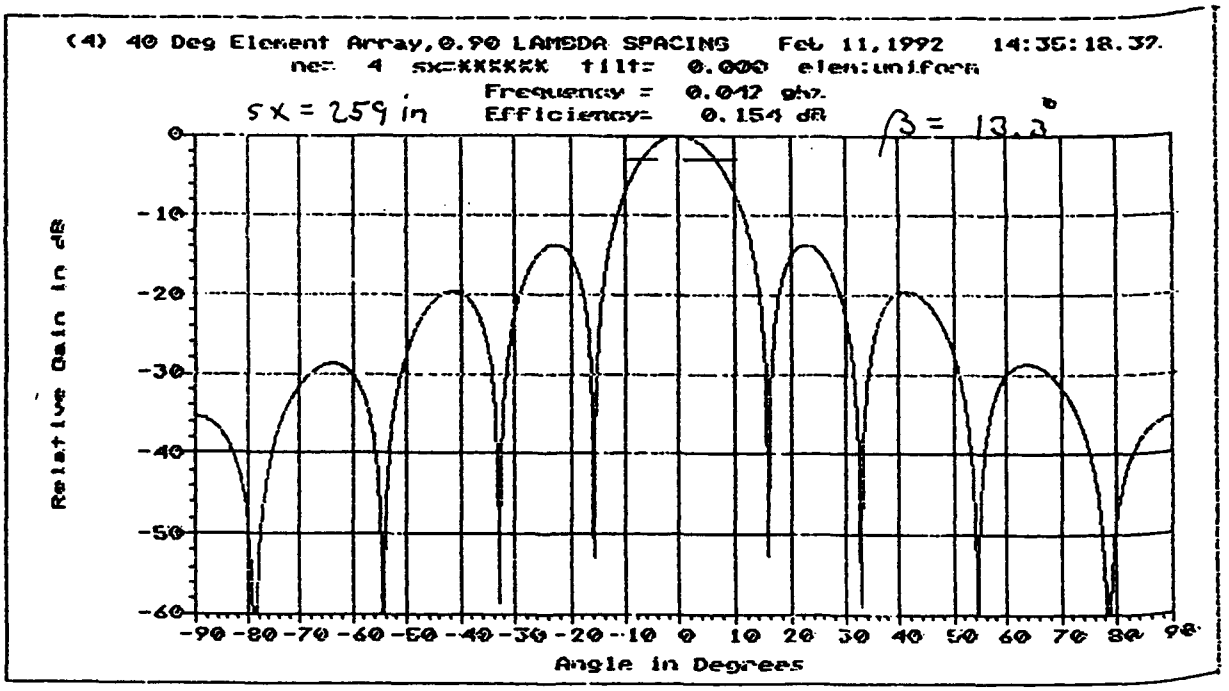

18.25dBi gain for 259 in spacing

19.2dBi gain for 288 in spacing (24ft)

Figure 13 Array Element Patterns (Continued)

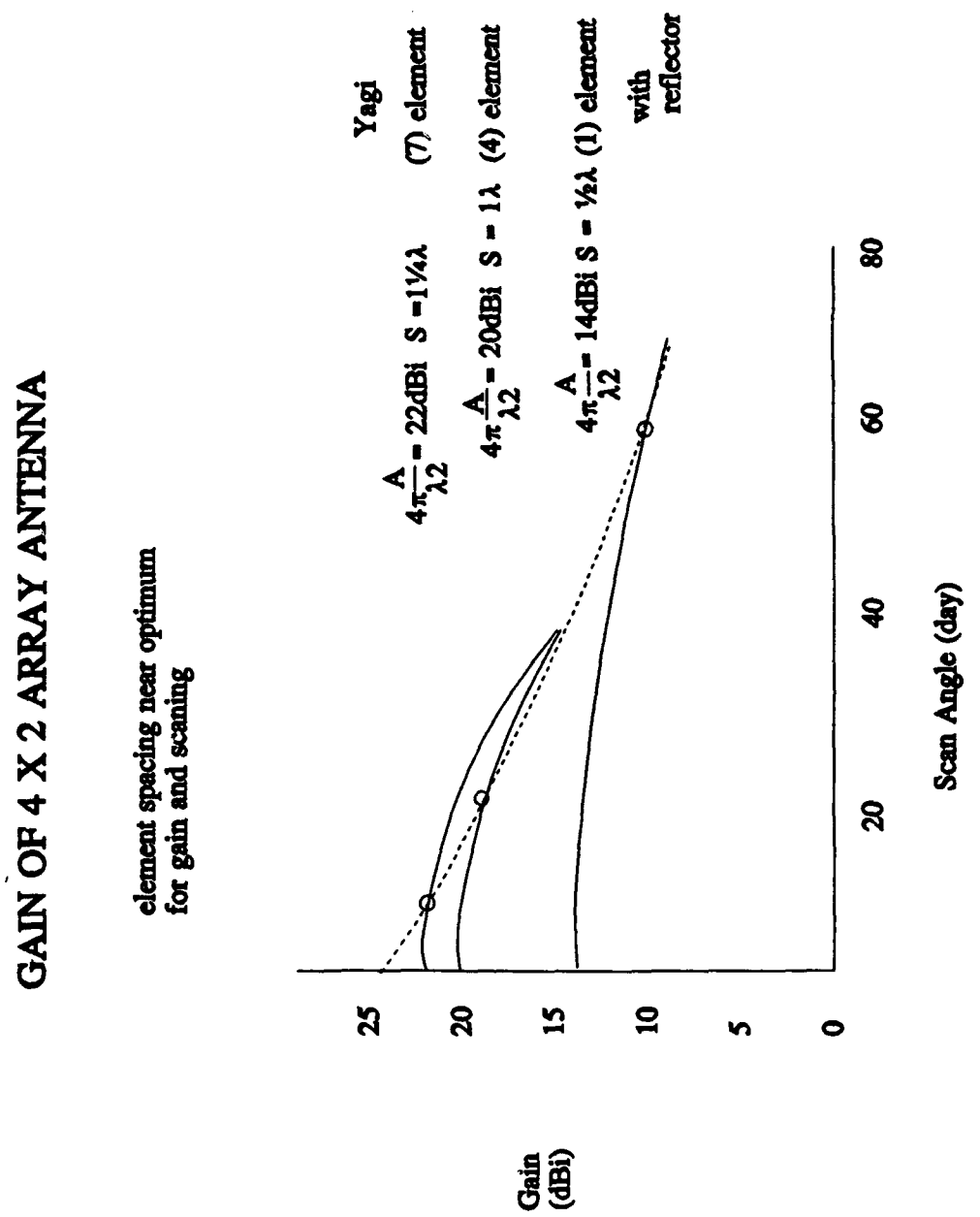

Figure 14 Gain of 4 x 2 Array Antenna

4.2 Installation Of The Nonadaptive Yagi Antennas

Fig.15 shows the placement of the high power amplifiers on the transmitter and the low noise preamplifiers at the base of the tower and following the phase shifters. A vector voltmeter is placed across the phase shifters and coupled to the antenna line through the directional couplers as in Figs.9 and15. The phase progression is set to the theoretical value derived in Fig.8 or to a modified value derived from calibration after antenna assembly. A calibration method is recommended in Fig.16 whereby the assembled antenna is illuminated with an external signal source placed about 170 ft out and 50 ft above the ground. The source would be offset from the antenna centerline by the required scan angle. The calculated phase shift setting would be modified in this calibration procedure to maximize gain in that direction. If this procedure does not give a phase progression somewhat near that expected, it is an indication that something is wrong. This precision is required by the relatively narrow azimuth beam width, which is on the order of 11 or 12 degrees depending upon the element spacing used. Fig.17 was made to show that this is a relatively large installation and to emphasize the precision needed to survey the antenna placement. That is, the base line of the array can not easily be moved once the antennas are installed.

Because the beam width is so narrow, the base line should be perpendicular to the great circle path to better than one degree. This accuracy must be achieved by a survey not based upon magnetic compass measurements. A preferred method would be based upon star position. For example, Figs. 18,19, and 20 show the North Celestial Pole to be about 0.8 degrees from the North Star, Polaris, in the direction of the end of the little dipper. This sequence of drawings shows the North Celestial Pole relative to the North Star. The first drawing is at low magnification so that one can be oriented relative to the Little Dipper. The following two drawings are then at higher magnification showing the direction of the 0.8 deg displacement of the North Star from the Celestial Pole. This would be a satisfactory reference procedure. The performance predicted for this path in TABLE II, for an average time of day and month of the year, is 6000 b/s throughput with a waiting time just under 30 sec. The gain of one Yagi antenna is 12.8 dBi. This is increased by 9 dB in the array so that the transmit and receive gains are 21.8 dBi. Transmitter power is 1200 W at each mast or 4800 W. This data is taken from the scaling model, BLINK, representing a first order estimate

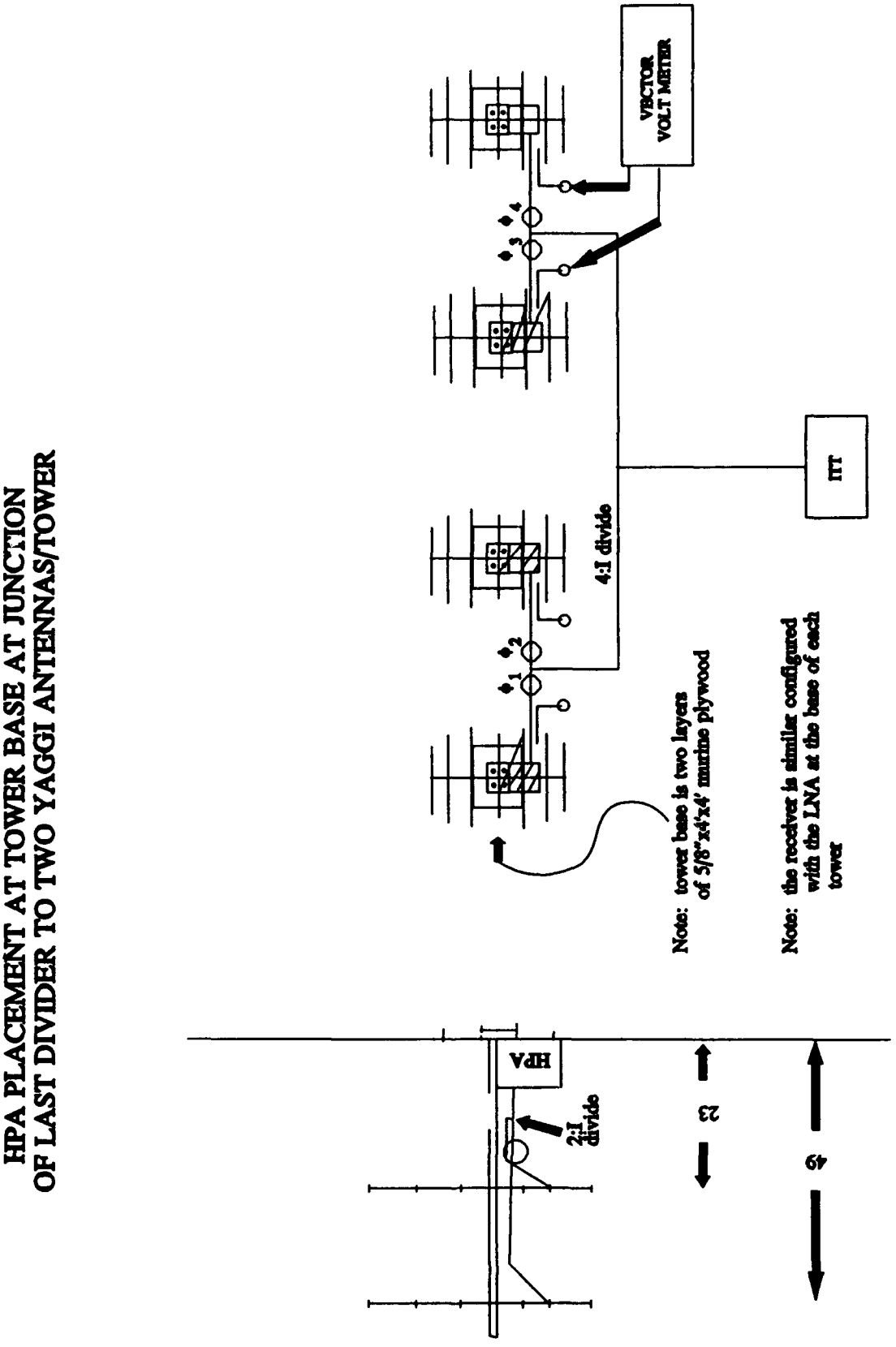

Figure 15 HPA Placement at Tower Base at Junction of Last Devider to Two Yaggi Antenna/Tower

GAIN AND POINTING CHECK

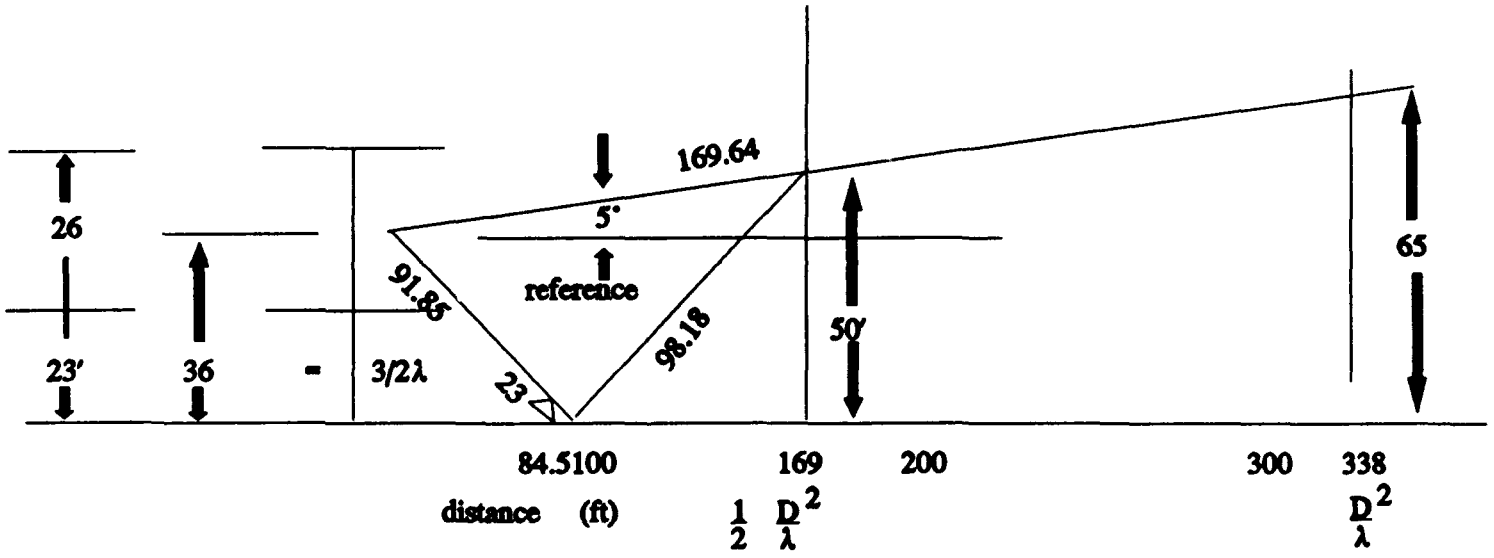

Figure 16 Gain and Pointing Check

at 1/2 W^2/λ Gain drop is 0.45 dB path difference = 169.6 - 91.85 - 98.18
First Side Lube is 9dB path difference = 20.43 ft
near null with 180° phase
reverse on reflection more out to 200 ft.

Aperture Width = 90 ft 1/2 W^2/λ = 168.8ft
Wavelength = 24 ft.
Need 50ft adjustable tower (portable)

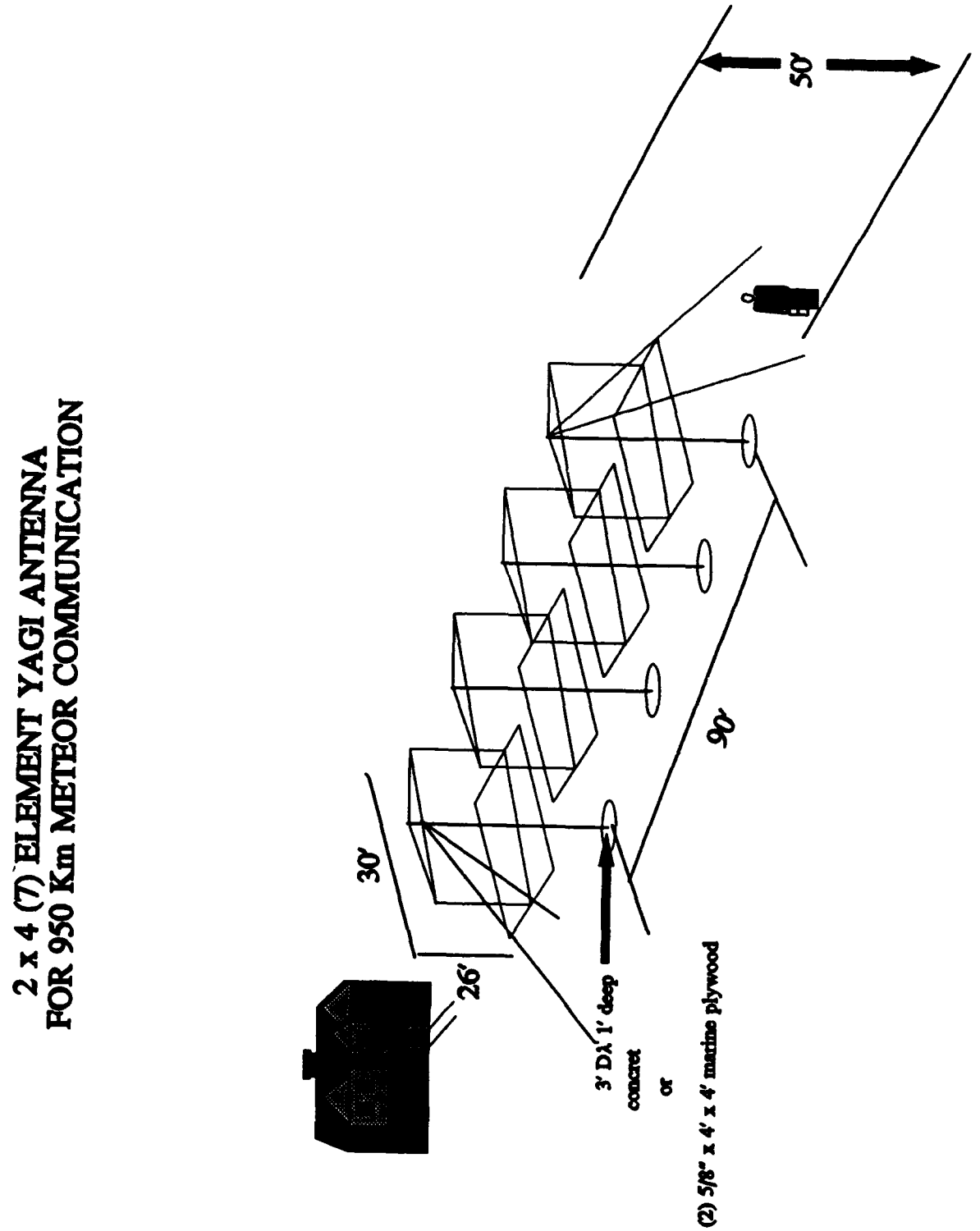

Figure 17 2 x 4 (7) Element Yagi Antenna for 950 Km Meteor Communication

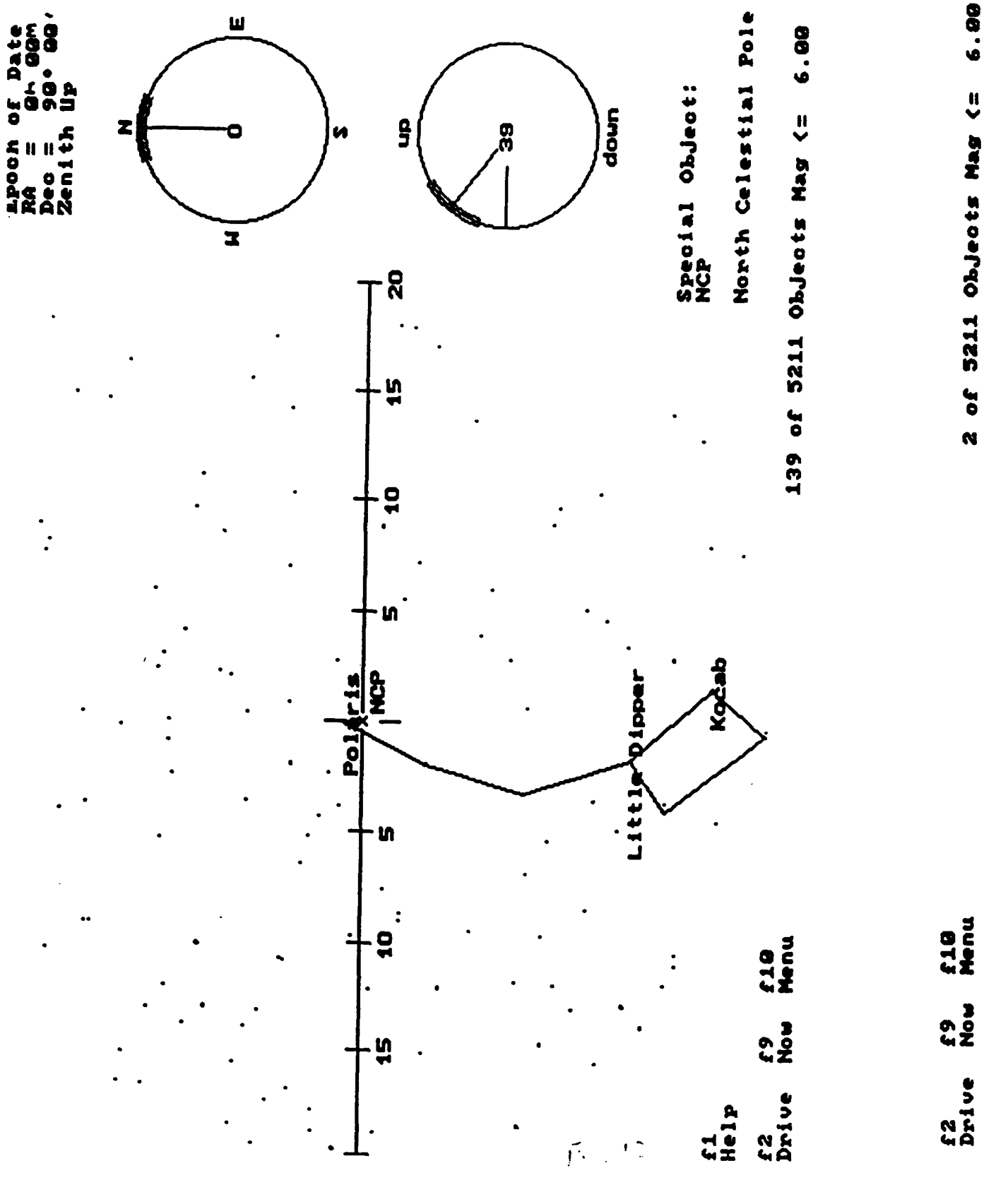

Figure 18 Calibration of MBC Antenna Subsystem Using Celestial Objects

of performance. Thus the high throughput could be demonstrated in July in a nonadaptive system.

4.3 Site Requirements For The Terminals Of The Nonadaptive Path

Site visits were made to Rome and Cherry Point, N.C. to establish the suitability of these locations. The requirements are listed in TABLE III. Rome is the preferred site for the receiver end as this should be the more radio quiet. RADC people made a rather careful spectrum survey in December, 1991 and found the received 41.0 MHz clear at that time. Here, also a housing for the receiver and processors is available as well as power. Less desirable but acceptable as a transmitter site is that at Cherry Point. The only location suggested by the Marine officer, frequency coordinator, is show in Fig.21 looking across a tree line with a 3.6 deg clearance. Power would be supplied by motor-generator and housing would be in a tent. There is plenty of room for the antenna placement.

TABLE 2.0 SITE REQUIREMENTS

Rome and Cherry Point

300X30 ft2 of ground space for antennas
5° unobstructed line of sight
rural background noise at 41.0 MHz
110 and 210 volts power for 20 KW of power
telephone (or cellular phone)
equipment housing
two man assembly crew
transit and nominal assembly tools
a head

Additionally at Rome

50 ft portable extending tower

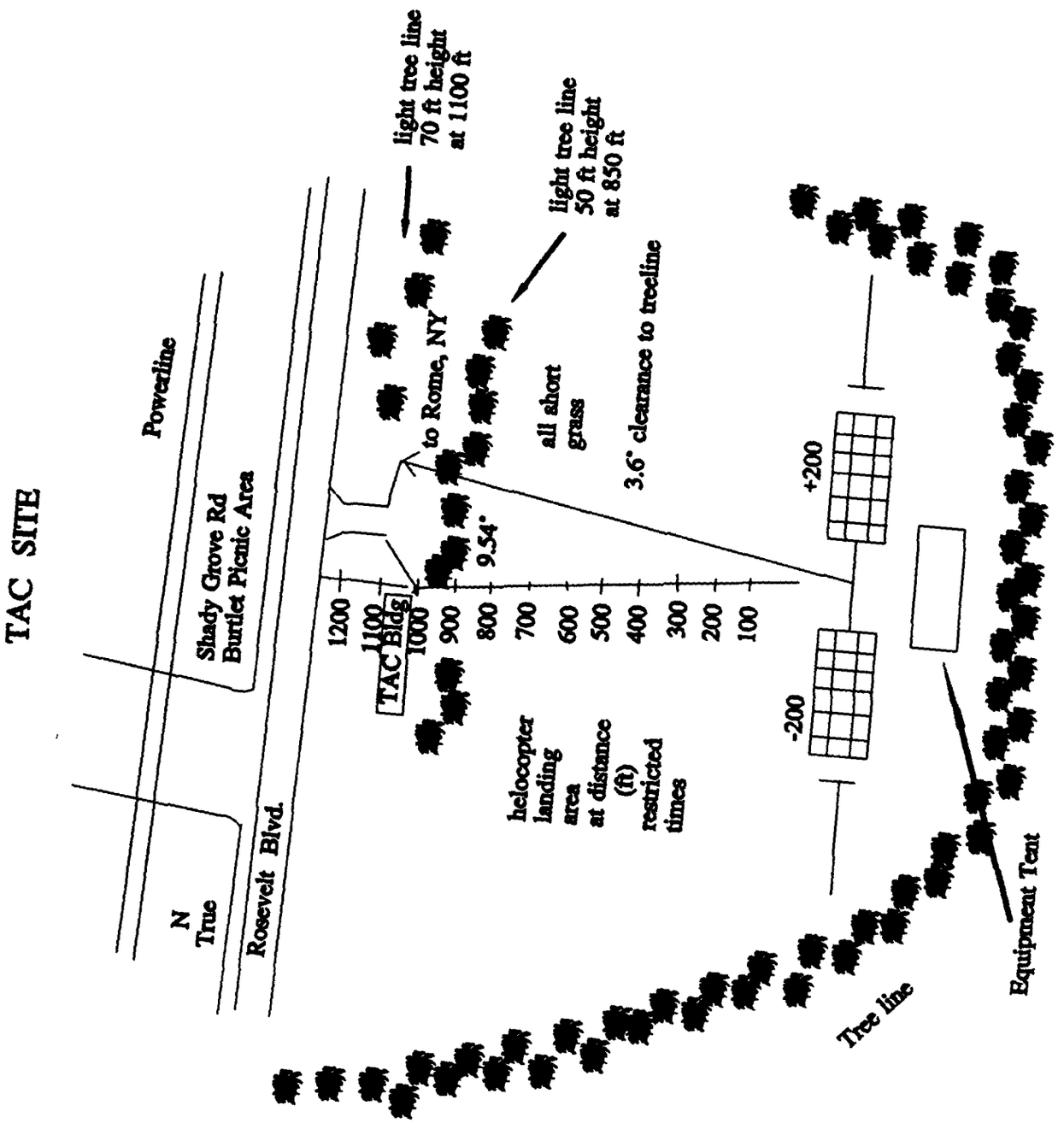

Figure 19 TAC Site

RADIATION AND EXPLOSIVE SAFETY

- Personnel exposure limit is 1.0 mw/cm^2 from 30 to 300MHz averaged over 6 mo. period. ANSI C95.4 "Radio Frequency Radiation Protection Guide:. This level is only exceed within the array itself.
- Electric-Explosive Device limit for most sensitive device is 2 V/m field strength. Air Force Standard AFR-127-100 "Explosive Safety: This level is exceeded only within the array itself.

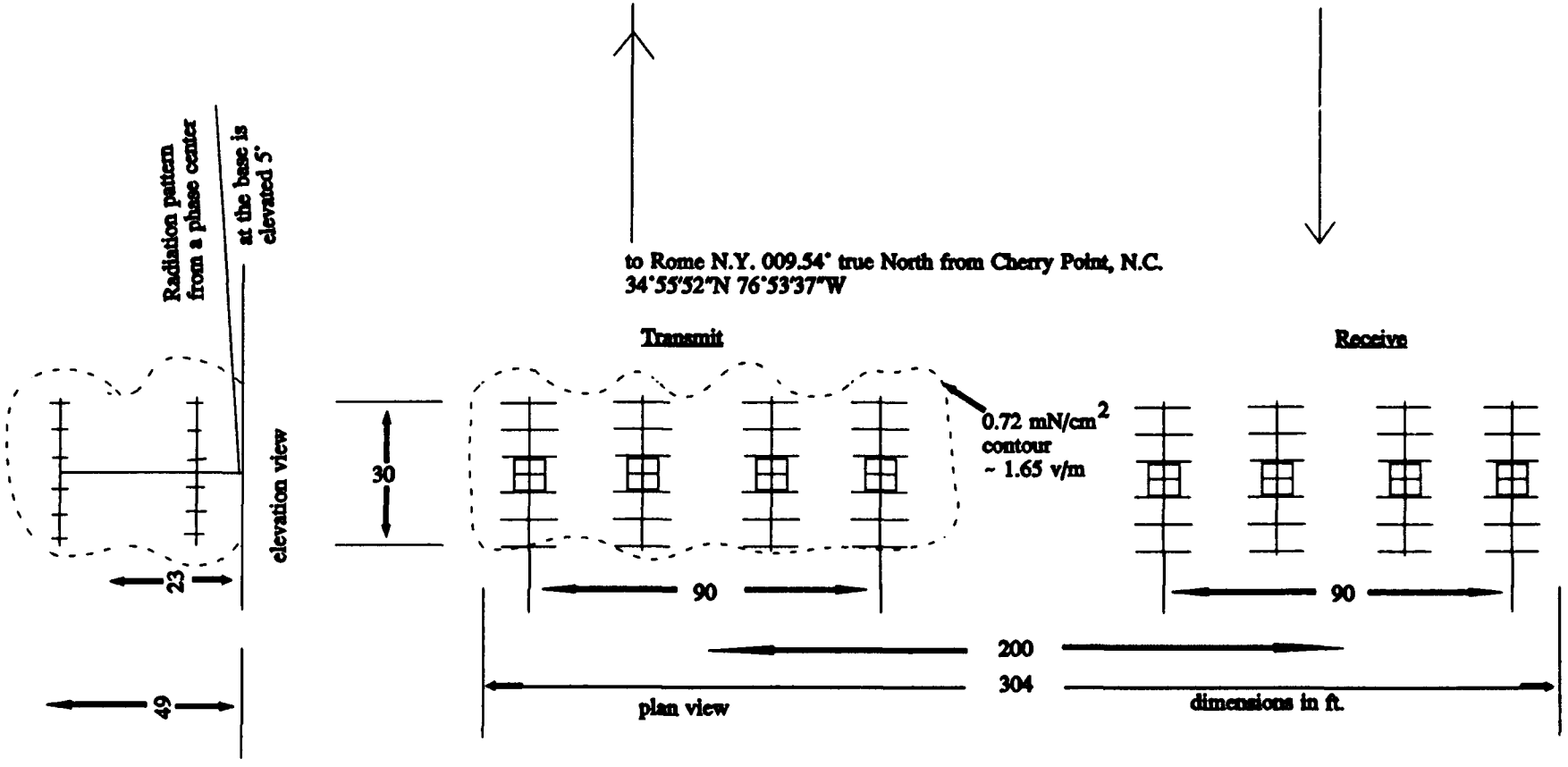

Figure 20 Radiation and Explosive Safety

P = 600 W/antenna $F_{Transmit}$ = 41MHz λ = 24 ft.

power density in effective aperture of each antenna = $\frac{P}{A} \quad \frac{600}{(24 \times 1.25 \times 12 \times 2.54)^2}$

Field ~ $\sqrt{120\pi P} = \sqrt{120\pi \times .72 \times 10^{-6} \times 100^2} = 1.65 V/m \quad P = 0.72 mw/cm^2$

There are questions concerning personnel safety and explosive safety in the presence of the 4.8 KW transmitter. The standard for personnel safety from ANSI C95 4 from 30 to 300 MHz averaged over a 6 month period is 1.0 mW/cm2. Assuming a plane wave front at the face of the array extended over the receive cross section as in Fig.10, the power density is 0.72 mW/cm2, a safe situation.

P = 600 W/antenna, F = 41 MHZ, Wavelength = 24 ft
antenna element aperture, A = 1.252 wave lengths square
power density in the effective aperture = p = P/A
p = 600/(24X1.25X12X2.54)2 = 0.72 mW/cm2

The Electric-Explosive Device limit for most sensitive device is 2 V/m field strength from Air Force Standard AFR-127-100 "Explosive Safety". This limit is exceeded at the aperture by a factor of 25 as follows:

field = (120_p)1/2 = (120_X0.00072X1002)1/2 = 52V/m

Thus, there is excessive power density for personal safety only within the antenna itself. The field strength does, however, exceed limits for most sensitive device at the antenna face and it would remain that way for 2.3 miles. A dotted contour is shown on Fig.22 representing the limit of 0.72 mW/cm2. This situation would have to be investigated further relevant to explosive storage.

As it became time for the purchase of the equipment for the nonadaptive high data rate test, two factors developed changing the Westinghouse participation in the contract. One was that the equipment cost had risen in the effort to achieve the high data rate so that it couldn't be covered by the contract, and the other was DARPA's continued interest in Westinghouse working on the adaptive antenna. As a result Westinghouse left the final selection of equipment and the purchase to SAIC. Their final block diagram and equipment list for the transmitter and receiver are given in Appendix A. They are essentially unchanged from the block diagram of Fig.9 and Table I, but most of the equipment suppliers are different. This information is included because it is necessary for interfacing the adaptive system to this apparatus at the completion of the nonadaptive high data rate test. In addition Appendix B is appended giving some details on the high data rate ITT modem as it is planned that the adaptive system would also interface with that modem. The versatility of the digital adaptive processor for not only this application but others, is described in the following section.

5.0 The Digital Adaptive Modem

5.1 Introduction

The digital adaptive system has been planned for 8 receiving channels at 41.0 MHz. This type of processing is difficult for a radar applications because of the high information rates, but here for communication, processing easily occurs in real time. It is being applied now for meteor communication, but it has application to satellite and to HF communication as well. Fig.23-26 show some of these applications. In Fig.23 the processor is used for a 4X2 array on a relatively long path for meteor communication representing the present application. For a short path the eight elements would be modified for wide angle coverage without other system changes as in Fig.24. For satellite communication in mobile vehicles using this eight channel processor, the elements become short axial mode helix antennas looking to the zenith as in Fig.25. At HF where one has a vertically polarized base station communicating omnidirectionally, the eight elements become vertical quarterwave monopoles as in Fig.26. From application to application, the preamplifiers change but the processor remains invariant. The system provides adaptive beamforming in two degrees of space without additional hardware, it identifies the carrier or its modulation as the signal, and suppresses other signals as noise by placing antenna nulls on the source. This is achieved in real time with about a 10 ms signal delay of the information such that no part of the signal is lost during a beam formation time.

5.2 Digital Adaptive Antenna For Meteor Burst

The upper section of the block diagram in Fig.38 represents a 4X2 array of antenna elements (4 in azimuth and 2 in elevation) followed by receivers and an adaptive processor. The antennas are 7 element Yagis spaced such that the beam can be directed about ± 25 deg in azimuth to cover the major meteor activity for a 950 Km path. The array beam is physically elevated about 12 deg above the horizon by antenna placement and scanned in elevation +20 by -5 deg. The beam scanning of course does not occur physically as would be measured on an antenna range, but rather it occurs in the processing of the data collected at each element from all directions covered by the antenna elements. Thus the element patterns must be wide enough to cover the scan volume just as in a physically scanned array.

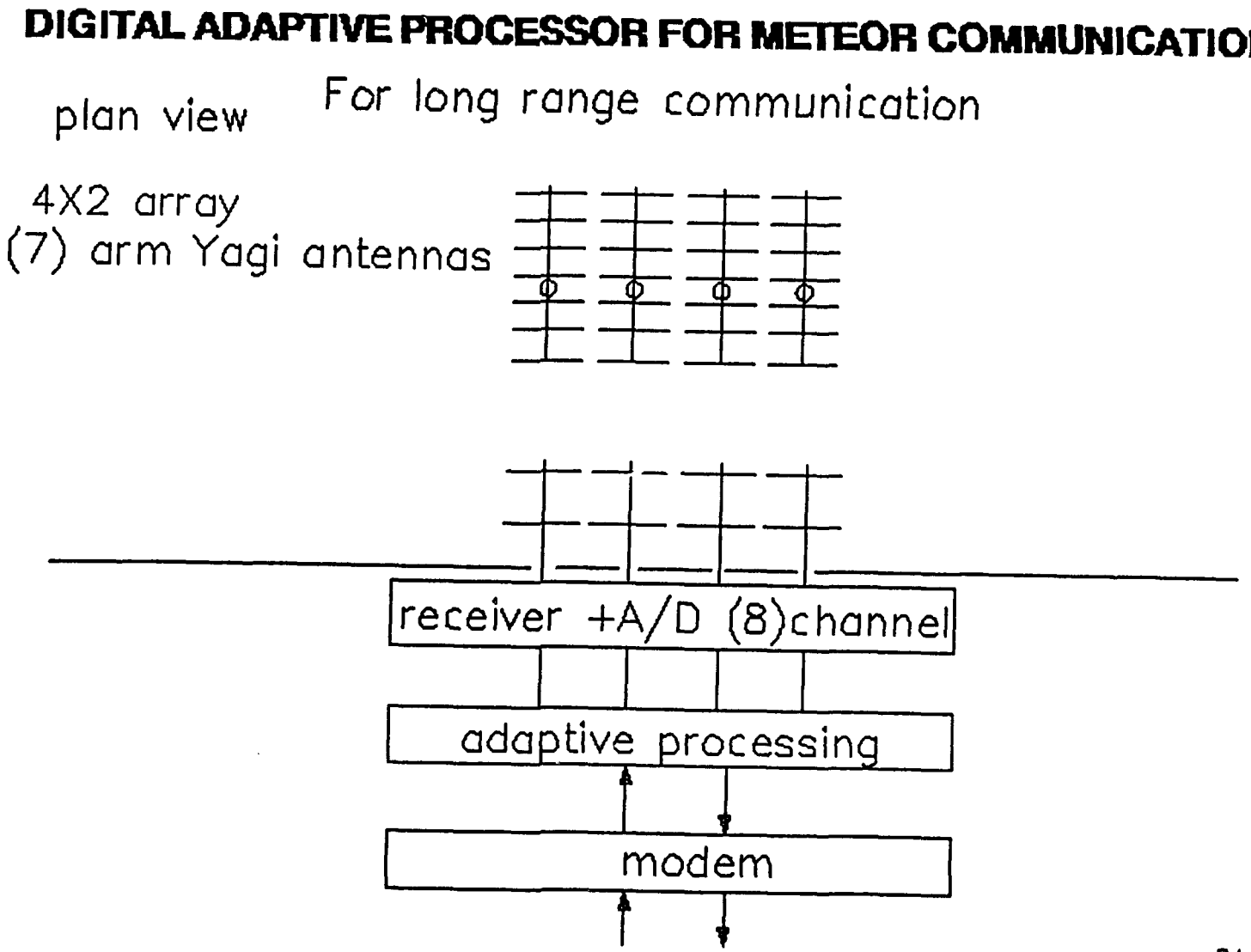

Figure 21 Digital Adaptive Processor for Meteor Communication

DIGITAL ADAPTIVE PROCESSOR FOR SATELLITE COMMUNICATION

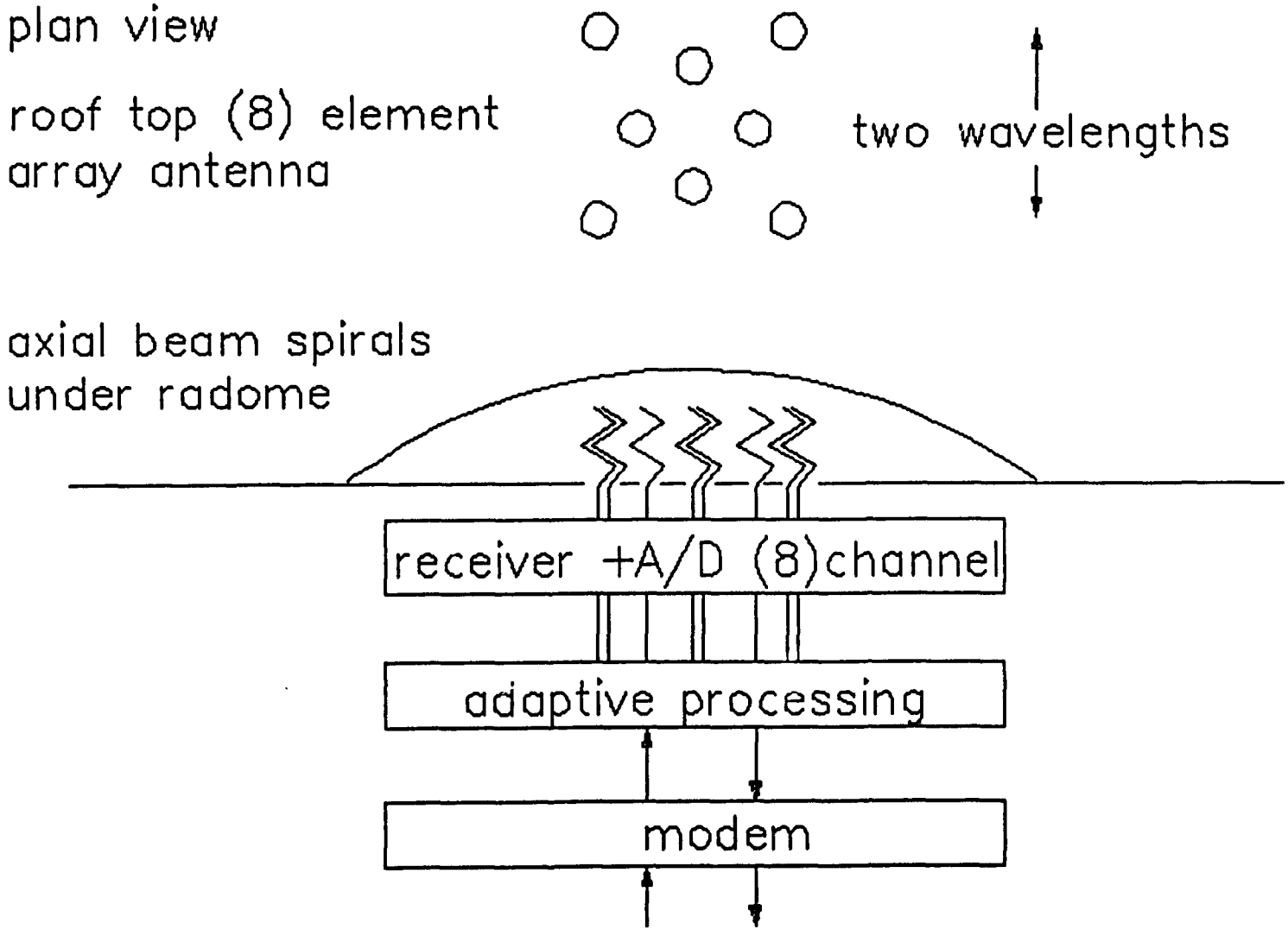

DAP 1
5/21/92

Figure 22 Digital Adaptive Processor for Satellite Communication

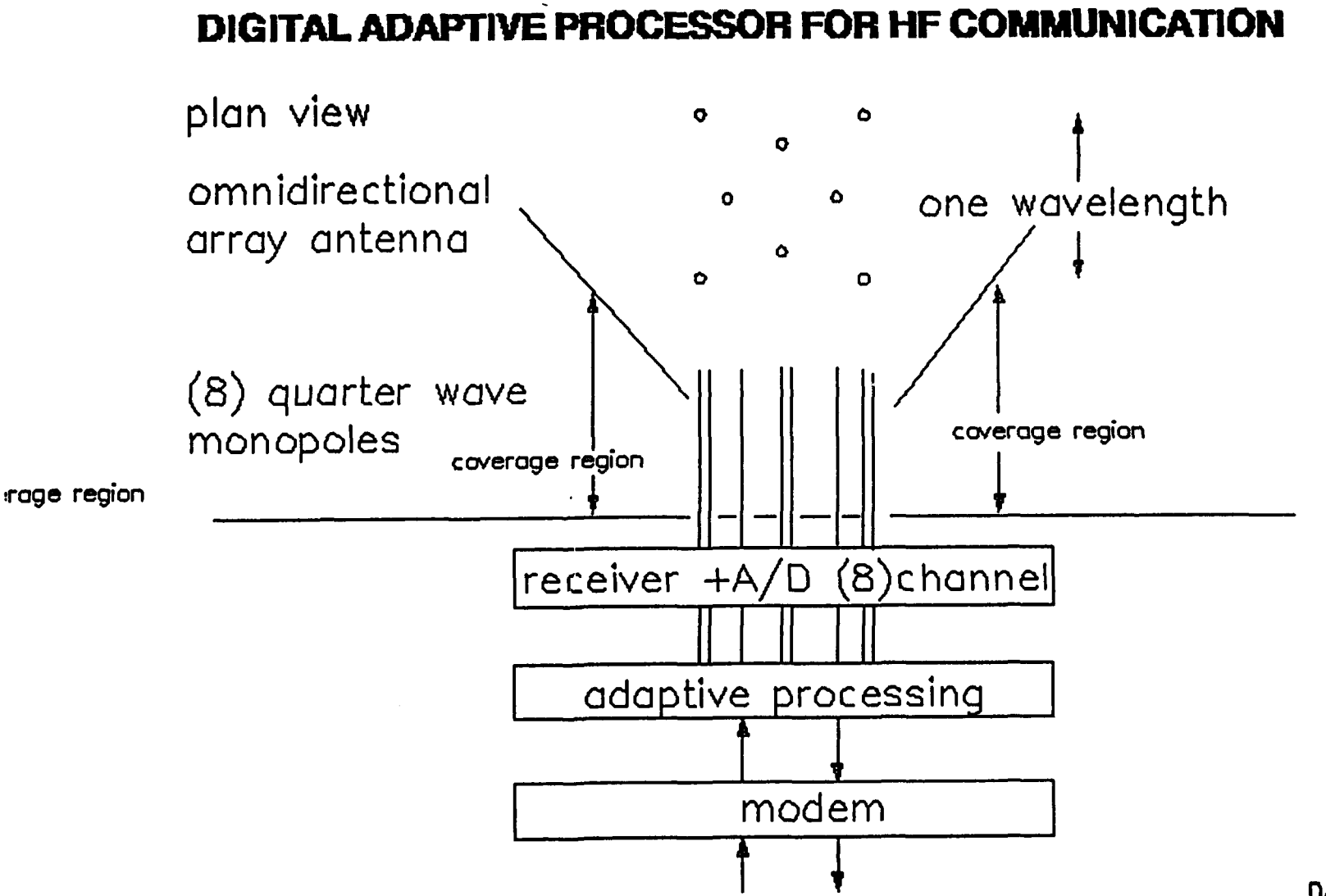

Figure 23 Digital Adaptive Processor for HF Communication

Following each antenna element is a bandpass filter centered at the 41.00 MHz carrier frequency and a low noise preamplifier. These will be in place and available for use, being part of the July measurements of the nonadaptive high data rate system.

At this point eight new double heterodyned receivers provide a signal level for A/D conversion. These are of high dynamic range and without AGC. Each channel is passed to the adaptive processor which may be considered in two parts, weight computation and weight application. Weight application is a phase and amplitude correction applied to each element to maximize the combined output signal-to-noise ratio. The signal must be correctly and uniquely identified so that other sources may be considered noise. In this sense the weights are calculated to provide the phase progressior or the array appropriate to the signal direction and nulls are set on strong interfering signals. At the same time phase and gain imbalance errors, that may have been introduced by amplifier channels or cable lengths, are automatically corrected. Each channel is shown buffer delayed, weighted and summed on the block diagram. The entire meteor signal is delayed on the order of 10 ms by this process, but no part of the burst is lost as the signal comes out of the noise, because the entire burst is similarly delayed.

The magnitude of the task for the envisioned 8 Kb/s data rate may be judged in that the above processing takes place on one DSP board in a PC as shown in the block diagram. In a complete modem, the signal would be demodulated and the meteor burst protocol handled on a second board. For this demonstration, the MB protocol is omitted as only a one way transmission of a broadcast signal is envisioned, to test the adaptive receiver performance.

The display on the block diagram shows signal strength of a given reflection against angle of arrival. The baseline display is a data point at the received direction and magnitude. Alternately the entire antenna pattern could be shown derived from the weighting function. This would be a relatively simple addition. The display need cover about a 70 dB range. Notice as an example, the strong reflection shown on the left at about -10 deg in azimuth with a null on an interference source near -3 deg. A weaker reflection at +18 deg fades into the noise sooner and also has a null at -10 deg. Several sequential reflections would be saved in this manner and then dropped.

The lower section of the block diagram represents the transmitterat Cherry Point. During the high data rate test in July, a 4X2 element array is being used for transmission, identical to the receive array. For this test, however, a broader beam transmitter is necessary to cover the meteor activity as no plans have been made to make the transmitter adaptive also. Thus, only one of the stacked pairs is activated in transmission to provide a 45 deg beam width.

5.3 Signal Strength Prediction For The Cherry Point To Rome Path

To center the dynamic range of the receiver design, it is necessary to calculate the upper end of the signal level expected from a reflection from an underdense reflection. This would represent near the maximum signal expected. The receiver dynamic range must handle all weaker returns down to the system noise floor. The following computation follows the notation of Shanker[3] following Sugar.

The division between underdense and overdense returns is usually taken as 1014 electrons per meter of trail. This number is used in Fig.28. A simplifying assumption is made in that relatively long path lengths such as the proposed 935 Km path have the meteor active regions concentrated near the great circle path as in Fig.1. Here the maximum reflection occurs for trails aligned with the great circle path and at midrange. Thus the cosine of the trail angle (beta) is unity as is the sine of the polarization angle, relative to the direction of propagation (alpha). The half angle of the reflection (phi) is

calculated to be 77.93 deg for a reflection at 100 Km altitude as in Fig.28. This maximum signal return is -70 dBm.

The minimum signal level is that available at the receiver noise level which at this frequency is -118 dBm determined from the 16 KHz band with a galactic noise at -160dBm/Hz at 41 MHz. This range of power levels is calculated in Fig.28 and graphed in Fig.29. A 70 dB dynamic range is set from -70 to -130 dBm.

Also on Fig.39 are the rural and residential noise levels that could prevail. Back ground noise peaks seen at Rome during a site visit during the winter of 91 are also shown with their indicated levels.

3. J.Z.Shanker, "Meteor Burst Communication", Artech House; Boston,London; 1990, pp 89-91.

Sections to be completed when the data is available

Signal strength statistics on the Cherry Point/Rome Adaptive System M.W.
Receiver design T.L.

6.0 Meteorburst Receiver Description

The eight channel receiver, MBCX-8, is shown in functional form in figure 1. Here we see eight identical receiver channels which take inputs from the antennas via the LNAs and connecting cables, (LNAs and cables are not shown and are not included as part of the receiver.) process down convert and digitize the signals to feed a digital multiplexer board and output to the processor (also not shown, nor included). Two stable crystal based sources are used to provide local oscillator signals and the A/D clock. Power is from 60 cycle/117vac via linear regulated ac/dc power supplies (included as part of the chassis).

Figure 2 shows more detail of the LO-generator, with the oscillators, clock divider, and output power dividers. Figure 3 functionally details the digital multiplexer board to provide clock drivers to each receiver, multiplexing of the digital data, and line drivers to the processor interface bus.

A spreadsheet analysis is shown in figure 4, outlining the various gains, noise figures and intermodulation distortions (third order intercept) numbers for each stage and cumulative. These figures have changed some since the original design, but they are close enough for design analysis. Figure 5 details the power supply requirements for each of the subunits in the receiver. Figure 6 is a parts list database of all of the ordered parts, most of which are in the receiver, a few of which were used for breadboard testing. (Note: all residual material and spare parts are included with the unit.)

Figure 7 and 8 are details of the receiver board, schematic and layout. Figure 9 is a schematic of the digital mux board. There follows in Appendix A collection of measured results of individual unit tests and some assembly tests. No complete integrated tests were completed because of end of contract and the lack of a processor. The receiver

appears to meet all desired goals for the eight channel Meteorburst Communications Experimental Receiver.

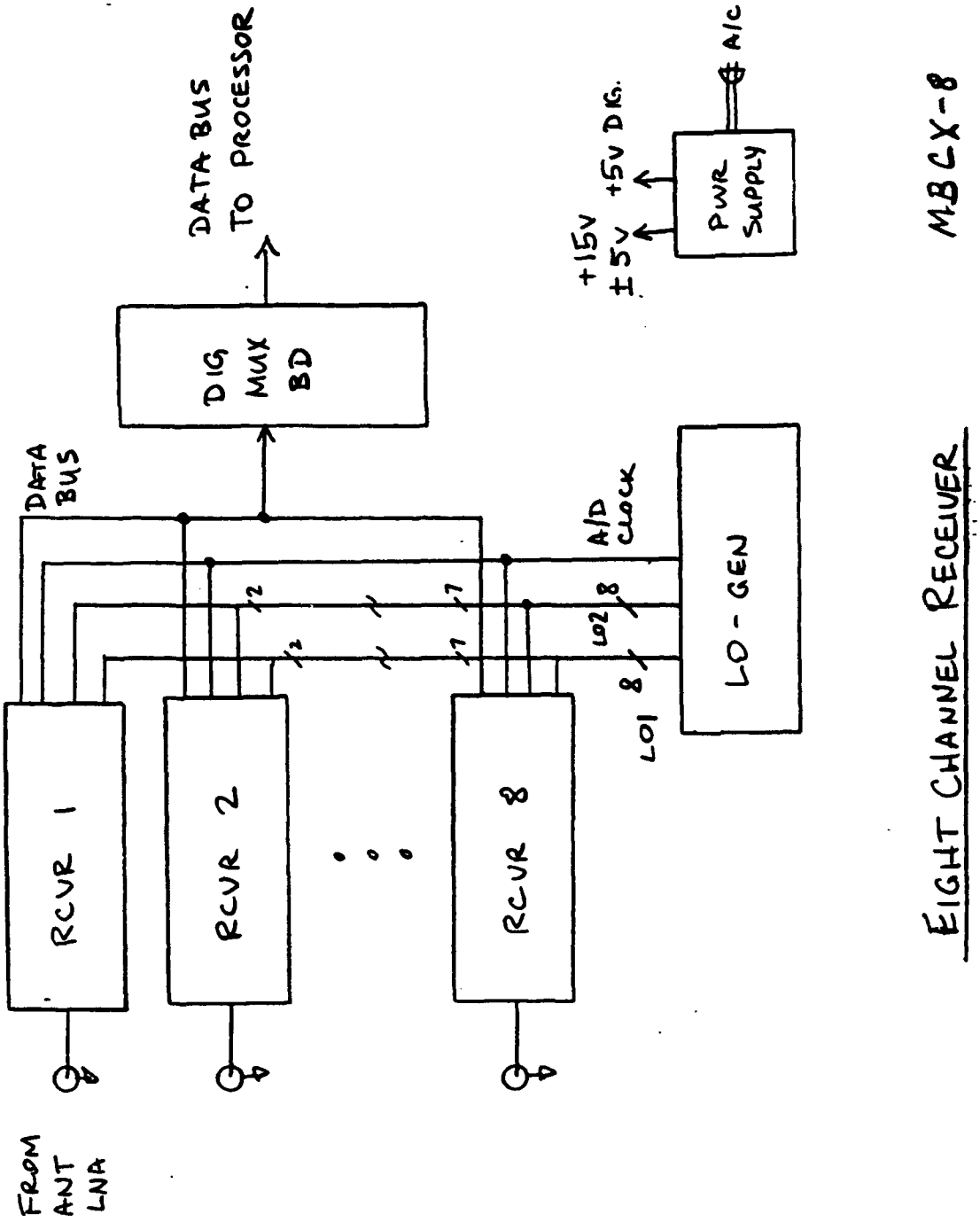

Figure 24 Eight Channel Receiver

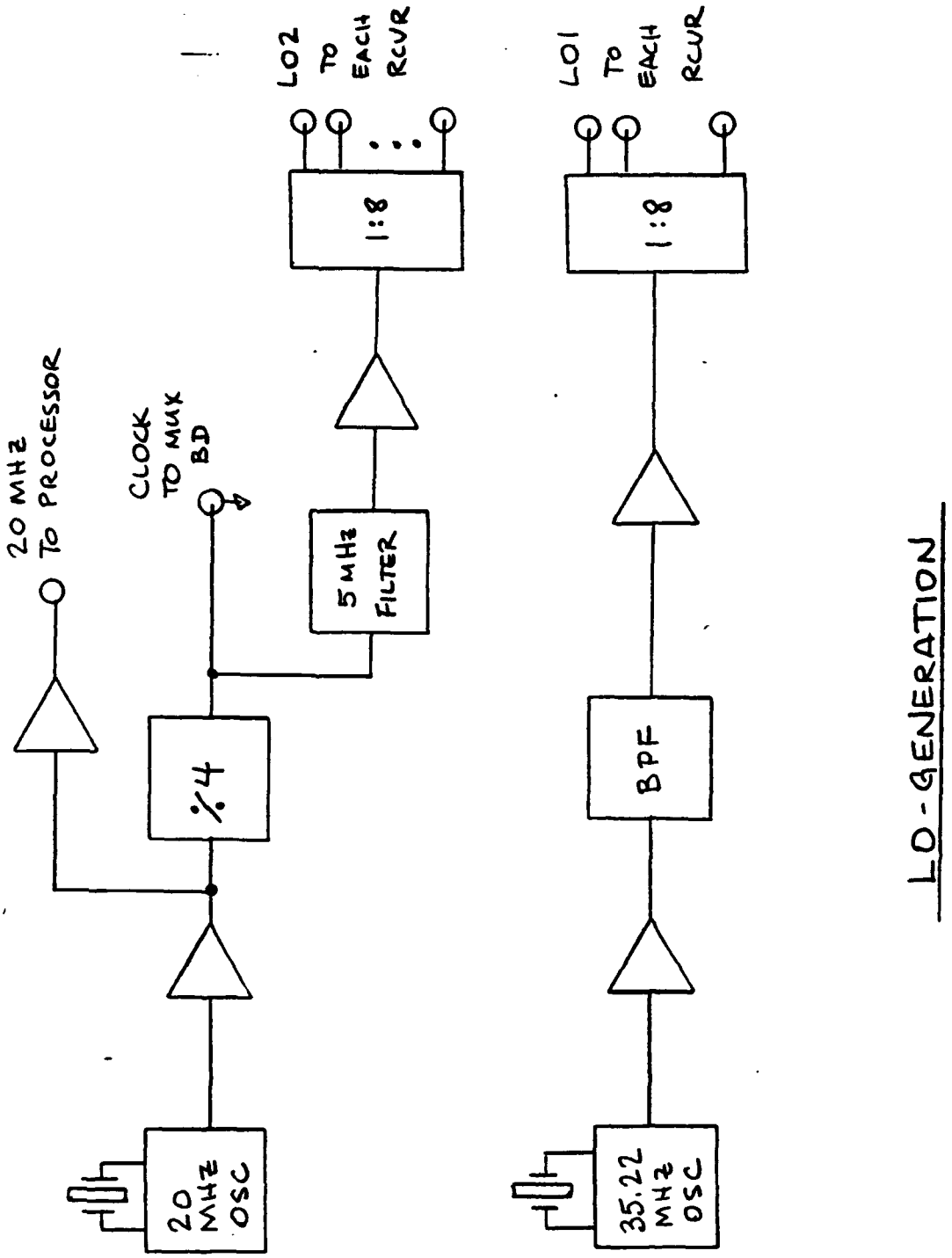

Figure 25 LO - Generation

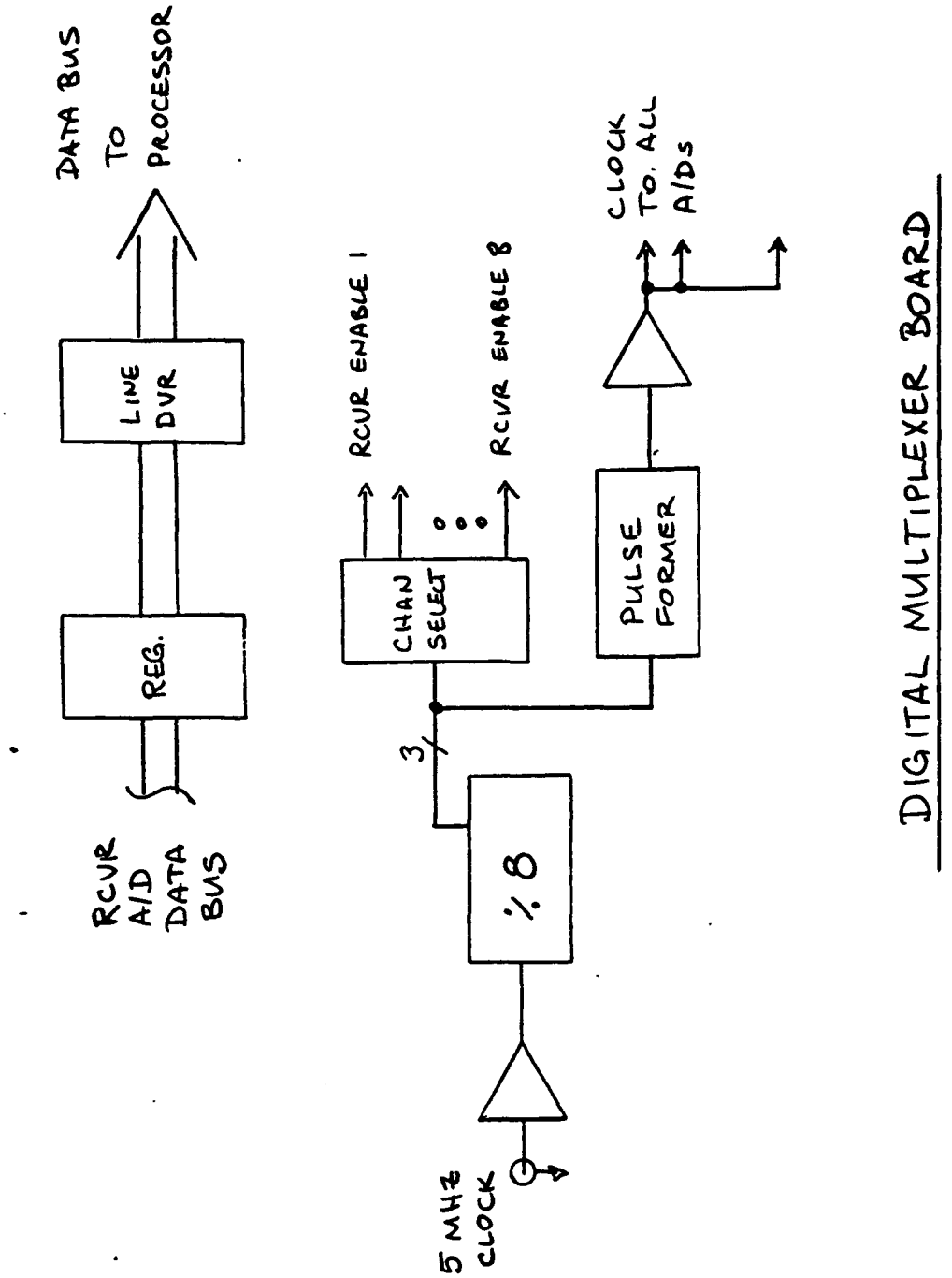

Figure 26 Digital Multiplexer Board

RCVRMET3.XLS 6/8/92

8-Jun-92 3:19 PM	STAGE GAIN dB	STAGE NF dB	STAGE IP3 dBm	CUM GAIN dB	CUM NF dB	EQUIV IP3 dBm	EQUIV InIP3	CUM IMP dBc	SIGNAL dBm
									-58.9
Prefilter	-2	2	50	-2.0	2.0	50.0	52.0	-233.8	-60.9
Rf LNA	19	2.4	28	17.0	4.4	28.0	11.0	-151.8	-41.9
Filter	-4	4	50	13.0	4.4	24.0	11.0	-151.8	-45.9
rf amplifier	19	2.4	28	32.0	4.5	27.9	-4.1	-121.5	-26.9
step atten	-4	4	50	28.0	4.5	23.9	-4.1	-121.5	-30.9
mixer	-6.3	6.3	30	21.7	4.5	17.3	-4.4	-121.0	-37.2
if amplifier1	19	2.4	32	40.7	4.5	30.8	-10.1	-109.7	-18.2
if filter	-3	3	50	37.7	4.5	27.8	-10.1	-109.6	-21.2
if amplifier2	15	3.3	32	52.7	4.5	31.6	-21.1	-87.7	-6.2
pad	-1	1	50	51.7	4.5	30.6	-21.1	-87.6	-7.2
if mixer	-5.8	5.8	30	45.9	4.5	23.8	-22.3	-85.3	-13.0
video filter	-4	4	50	41.9	4.5	19.8	-22.3	-85.3	-17.0
pad	-1	1	50	40.9	4.5	18.8	-22.3	-85.3	-18.0
video amp	30	10	50	70.9	4.5	48.3	-24.6	-80.5	12.0
ADC	0	68.00	48	70.9	5.2	43.1	-27.8	-74.2	12.0

	1.4	QRMS set level		60.4 dB Dynamic Range (SampleBW)
	0.6	QRMS internal	-4.43697	
	12	dBmFS		
	12	BITS	-51.24	
	0.1	MHzSampleBW	-10	
	68	NF dB		
GAIN REQD:	71.2	dB	60.3503	

Figure 27 RCVRMET3

Unit	Part Number	Qty/Unit	5 V ana	-5 V ana/dig	15 V ana	5 V dig
8	Receiver					
Step Atten	TOAT-51020	1	10			
Amp	AMP-75	2			29	
Amp	AMP-77	3			56	
Video Amp	AD9617JN	1	40	40		
ADC	AD1671JD	1	60	60		5
Register6	74LS378	2				18
Total Current Per Channel			110	100	226	41
Total Current for 8 Receivers			880	800	1808	328
	LO Generator					
10 MHz Osc		1				*50*
Crystal	35.22 MHz	1				*50*
Buffer	MC10116	2		20		
FlipFlop	MC10131	1		50		
Amp	AMP-77	2			56	
Total Current for Unit			0	90	112	100
	Multiplex Assembly					
Counter4	74LS161	1				26
Levelshift	MC10125	1		40		52
Decoder8	74LS138	1				8
Register8	74LS374	2				34
Linedrivers	26LS31	4				60
Total Current for Unit			0	40	0	394
Line Driver Terminations						800
Total Current for System (including line drivers)			880	930	1920	1622

Figure 28 Power

PARTLST2.XLS

Print Date:
8/16/92 2:28 PM

Part Number	Part	Vendor	PO Number	Placed	Stat	W/S Date	R.P.	Buy	Loc	Qty
CR76A/U	Crystal	Vargas Elec	K 42332	7/21/92	40	8/31/92	7/17/92	KB		2
2579	N/SMA	Midwest Micr	K 42333	7/17/92	60	7/30/92	7/17/92	RE	T-2	8
IO-IM-031721	Rack Frame	Optima	K 42334 A	7/20/92	60	7/29/92	7/17/92	HW	T-2	1
IO-IM-RA03	Rack Adapt	Optima	K 42334 B	7/20/92	60	7/29/92	7/17/92	HW	T-2	1
IO-IM-P-0317	Panels	Optima	K 42334 C	7/20/92	60	7/29/92	7/17/92	HW	T-2	2
IO-IM-TV-21	Vented Top	Optima	K 42334 D	7/20/92	60	7/29/92	7/17/92	HW	T-2	1
TOAT-51020	Step Attn	Mini-Circuits	K 42335	8/5/92	60	8/12/92	7/17/92	KC	T-2	9
AMP-75	Amp	Mini-Circuits	K 42336	7/24/92	60	7/31/92	7/17/92	KG	T-2	27
AMP-77	Amp	Mini-Circuits	K 42337	7/24/92	60	7/31/92	7/17/92	KG	T-2	27
LRMS-1H	Mixer	Mini-Circuits	K 42338	7/24/92	60	7/28/92	7/17/92	KG	T-2	18
KAT2	Pads	Microcraft	K 42339		20		7/17/92	EL		8
AD9617JN	Video Amp	Analog Device	K 42340		20		7/21/92	KG		8
ZFSC-8-1-S	Power Split	Mini-Circuits	K 42348	8/5/92	60	8/12/92	7/22/92	Z5	T-2	3
AD1671JD	ADC	Analog Device	K 42341	7/20/92	40	8/28/92	7/17/92	KZ		9
CTX114	10 MHz Os	Digi-Key	K 42342	7/21/92	60	7/31/92	7/20/92	KB	T-2	2
MC10116P	Line Rcvr	Hamilton	861146278	?	60	7/28/92	?	HC	T-2	2
MC10131P	D FF	Hamilton	861146278	?	60	7/28/92	?	HC	T-2	3
SN74LS378N	Hex FF	Hamilton	861146278	?	60	7/28/92	?	HC	T-2	20
SN74LS161AP	4 Bit Ctr.	Hamilton	861146278	?	60	7/28/92	?	HC	T-2	2
MC10125P	ECL>TTL	Hamilton	861146278	?	60	7/28/92	?	HC	T-2	2
SN74LS138N	Decoder	Hamilton	861146278	?	60	7/28/92	?	HC	T-2	2
SN74LS374N	Octal FF	Hamilton	861146278	?	60	7/28/92	?	HC	T-2	3
HC15-3-A	Power Sup	Power One	K 42354	7/31/92	60	8/16/92	7/28/92	EL	T-2	1
HAA5-1.5/OVP-A	Power Sup	Power One	K 42355	7/31/92	60	8/16/92	7/28/92	EL	T-2	1
HB5-3/OVP-A	Power Sup	Power One	K 42356	7/31/92	60	8/16/92	7/28/92	EL	T-2	1
PAL C22V10L-25PC	PAL	Cypress			60				mp	8
4116R-001-390	Res. Net	Bourns			60				T-2	36
SN74LS374N	Octal FF	Hamilton			60				T-2	18

Figure 29 Parts List

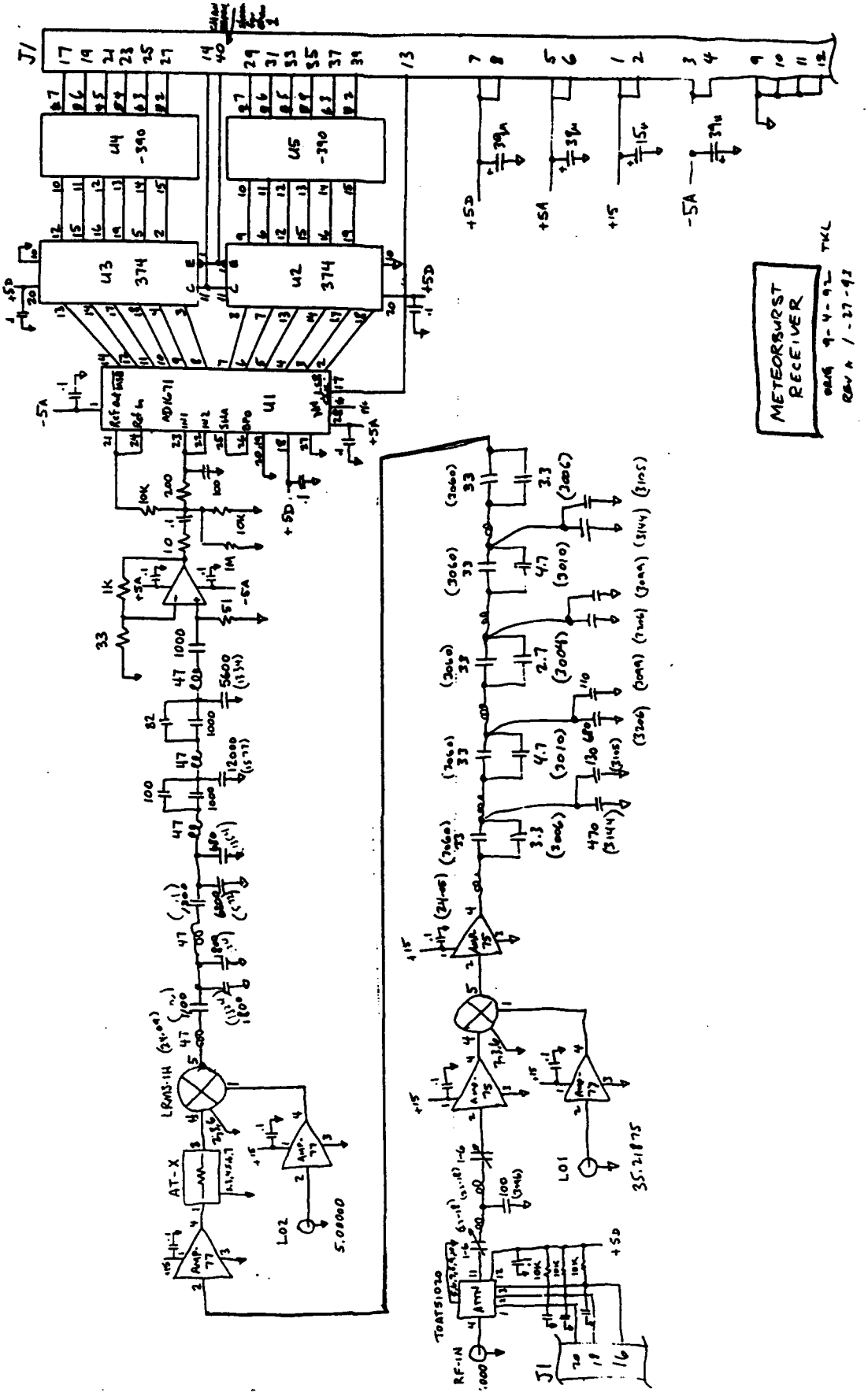

Figure 30 Meteorburst Receiver

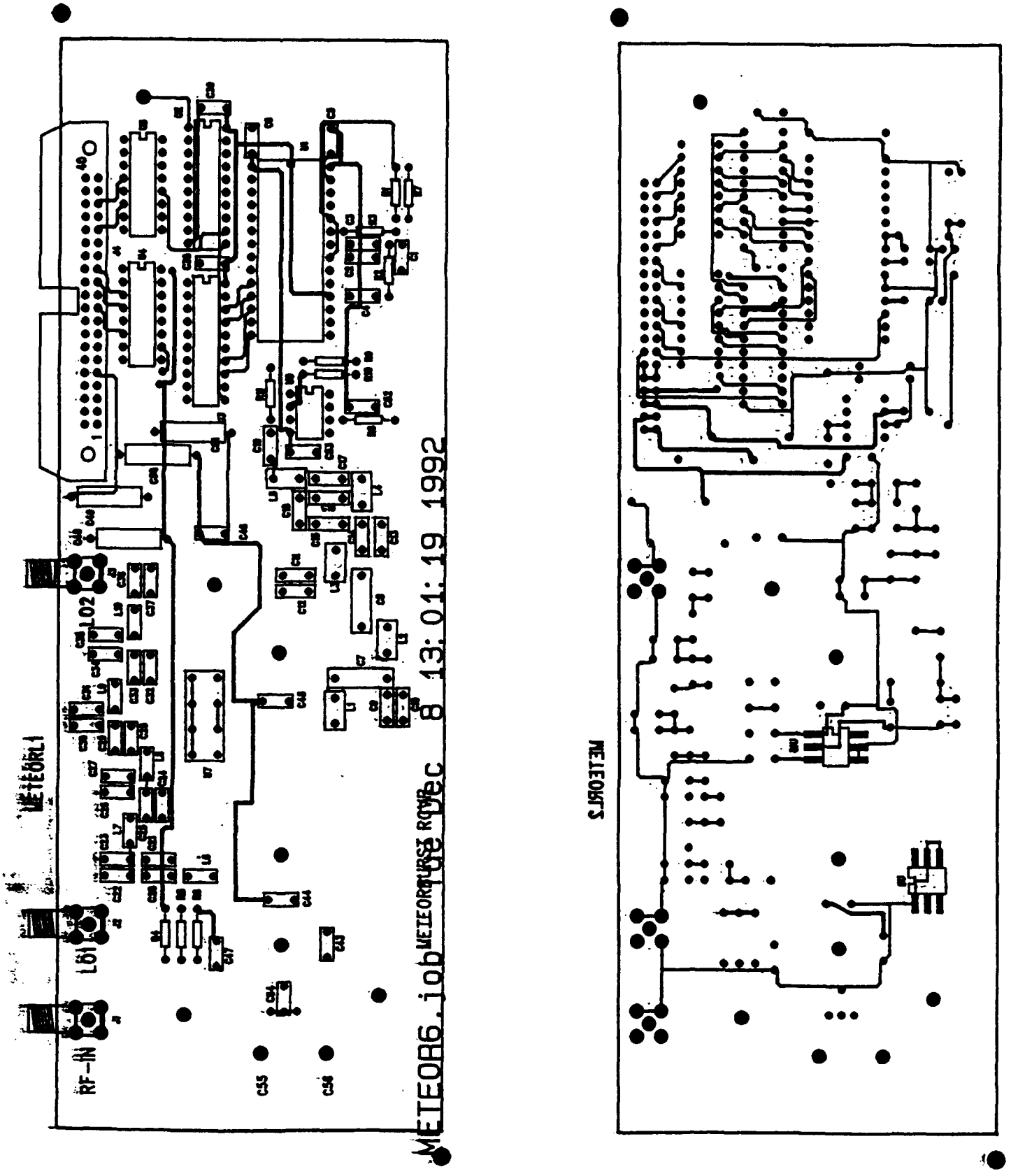

Figure 31 Meteorburst Receiver (Continued)

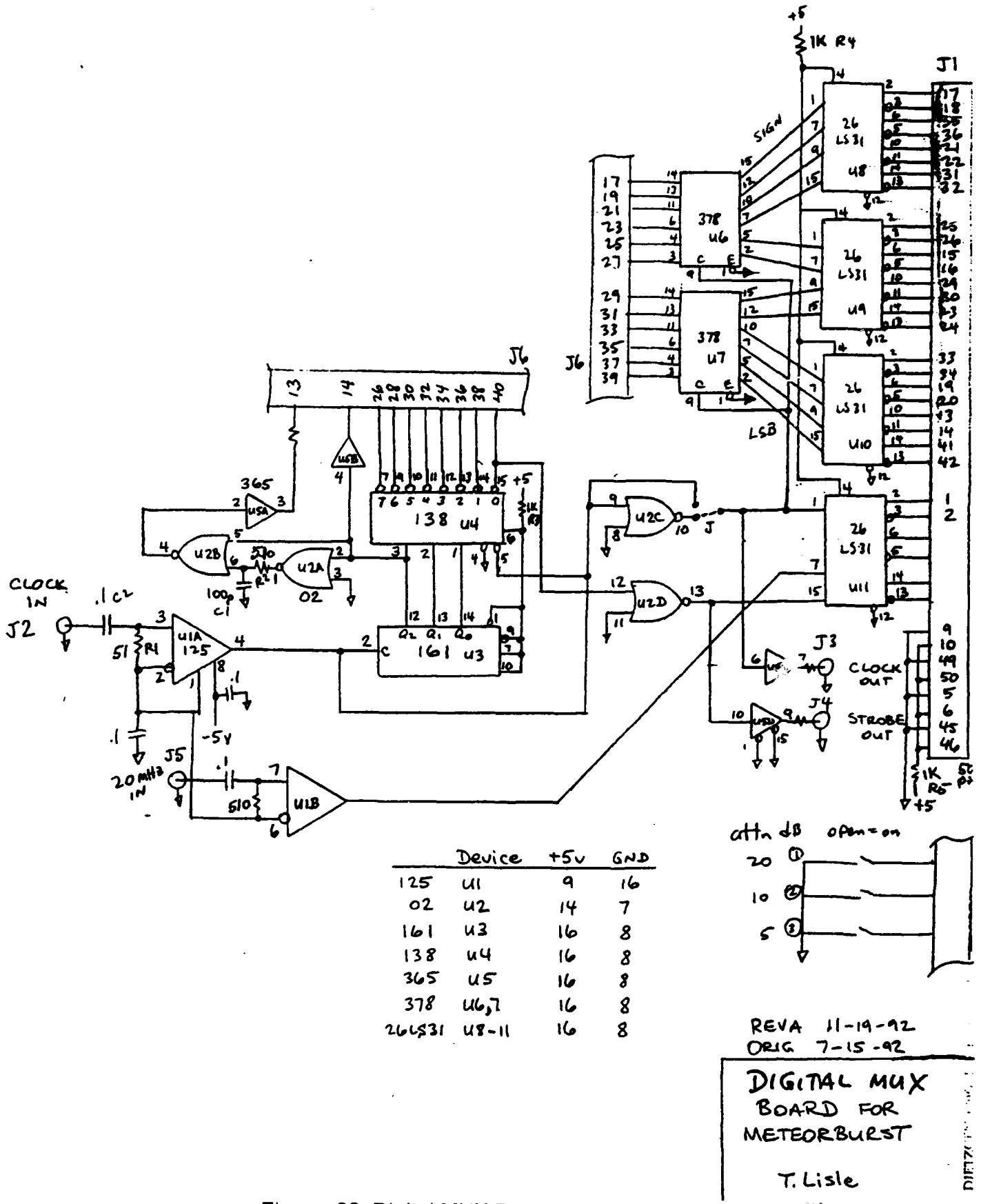

Device		+5v	GND
125	U1	9	16
02	U2	14	7
161	U3	16	8
138	U4	16	8
365	U5	16	8
378	U6,7	16	8
26LS31	U8-11	16	8

Figure 32 Digital MUX Board for Meteorburst

Appendix A, Various Measured Results

Receiver third order intercept data and linearity T.L.
Predicted and measured waiting time and throughput M.W.
Statistics on angle of arrival M.W.
Interference nulling performance D.P.
The digital processor M.P.
Conclusion M.W.

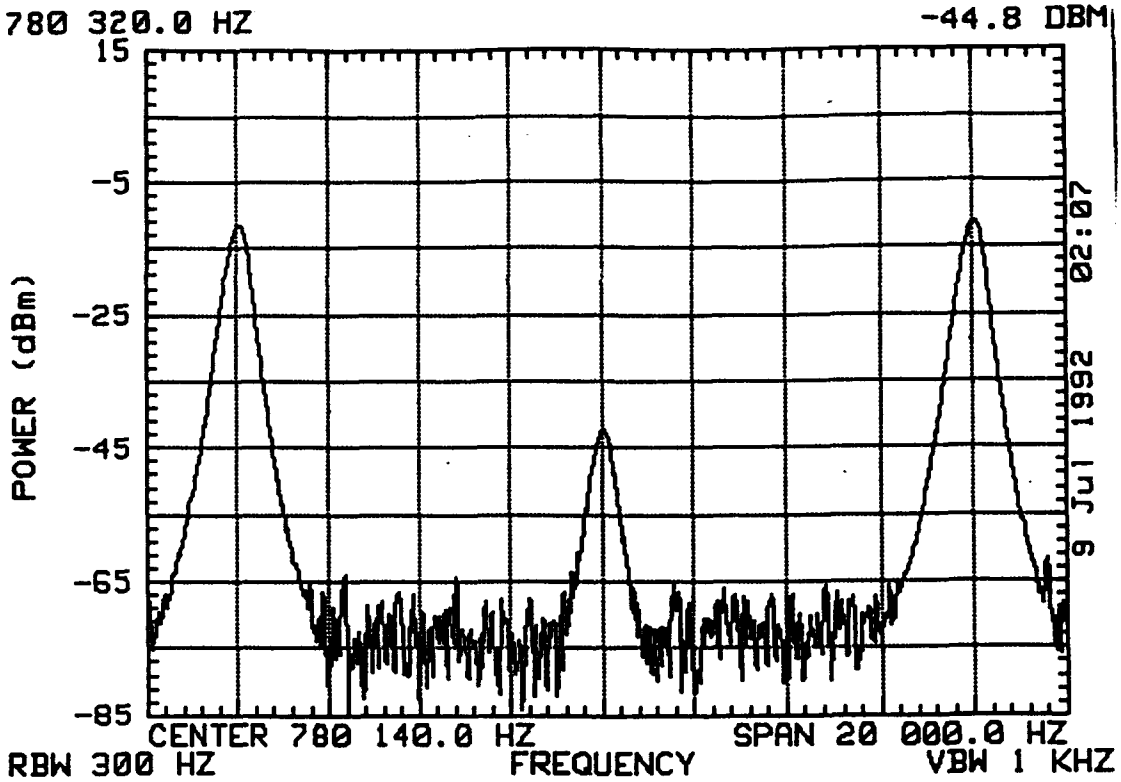

8kHz
BPSK
-80 dBm

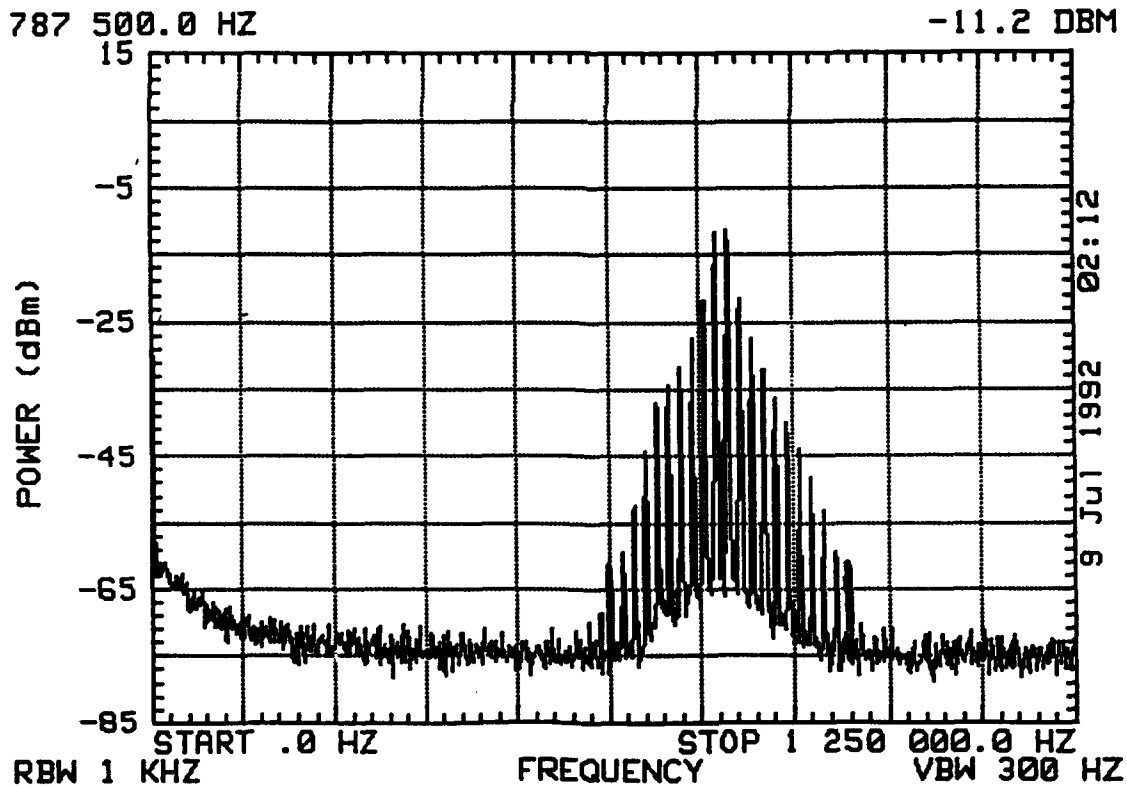

Figure 33 Various Measured Results 8kHz BPSK -80dBm

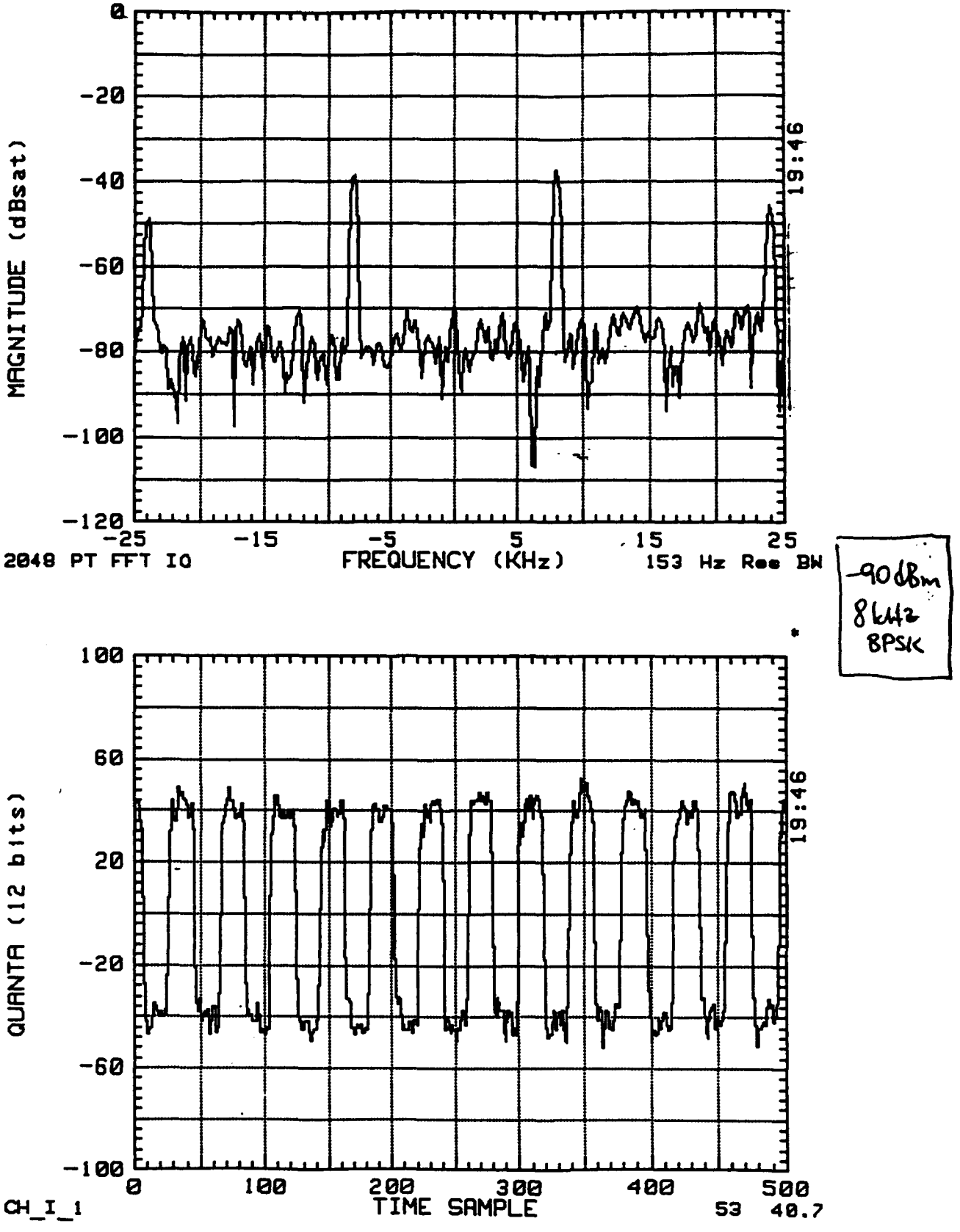

Figure 34 Various Measured Results -90dBm 6kHz BPSK

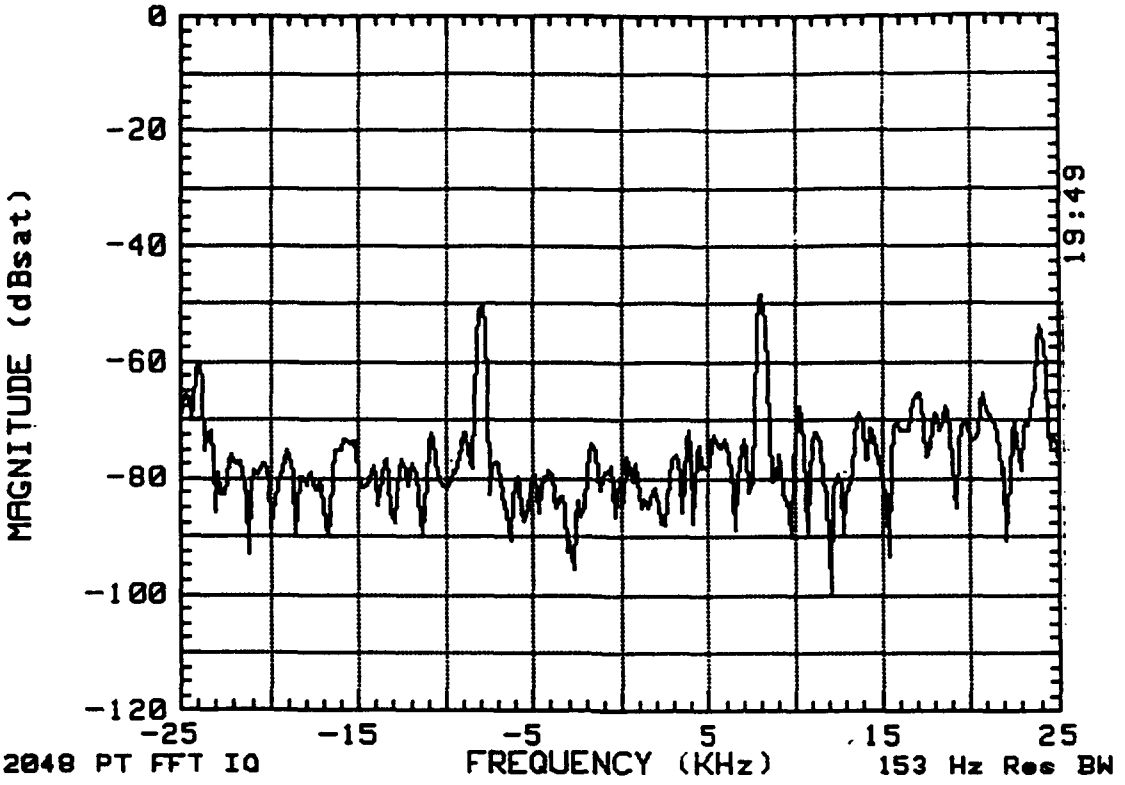

-100dBm
8kHz
BPSK

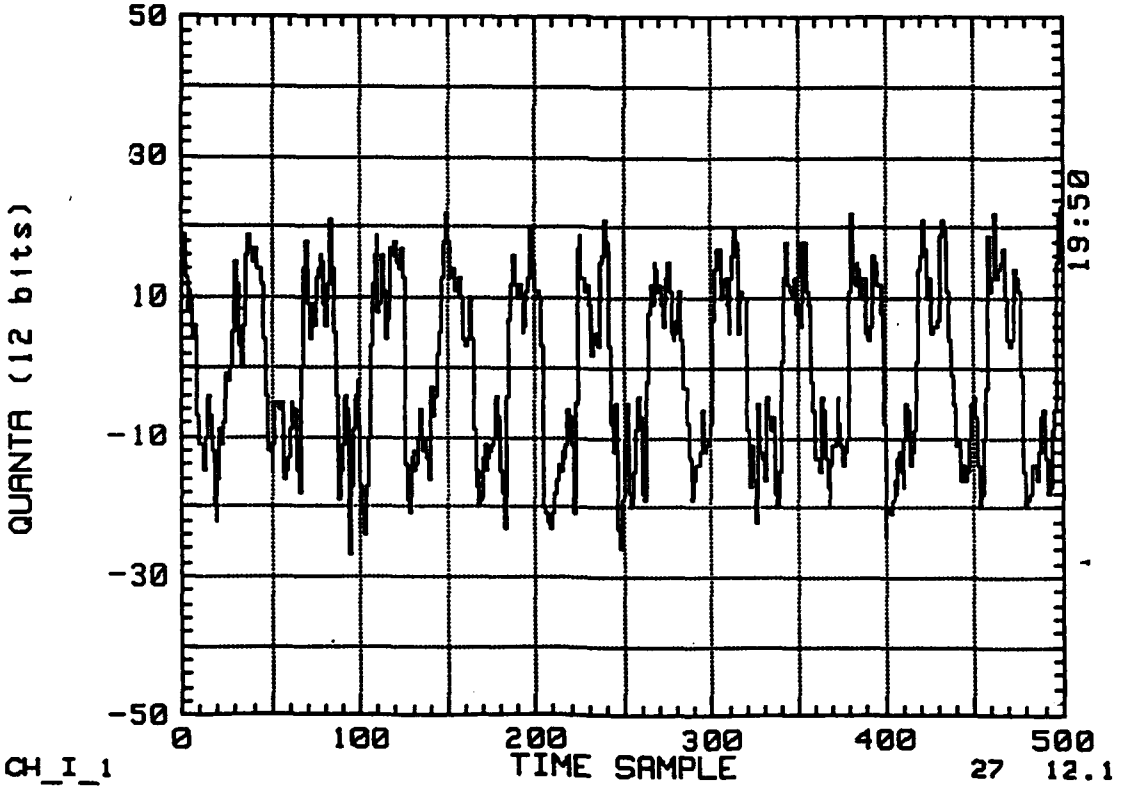

Figure 35 Various Measured Results -100dBm 8kHz BPSK

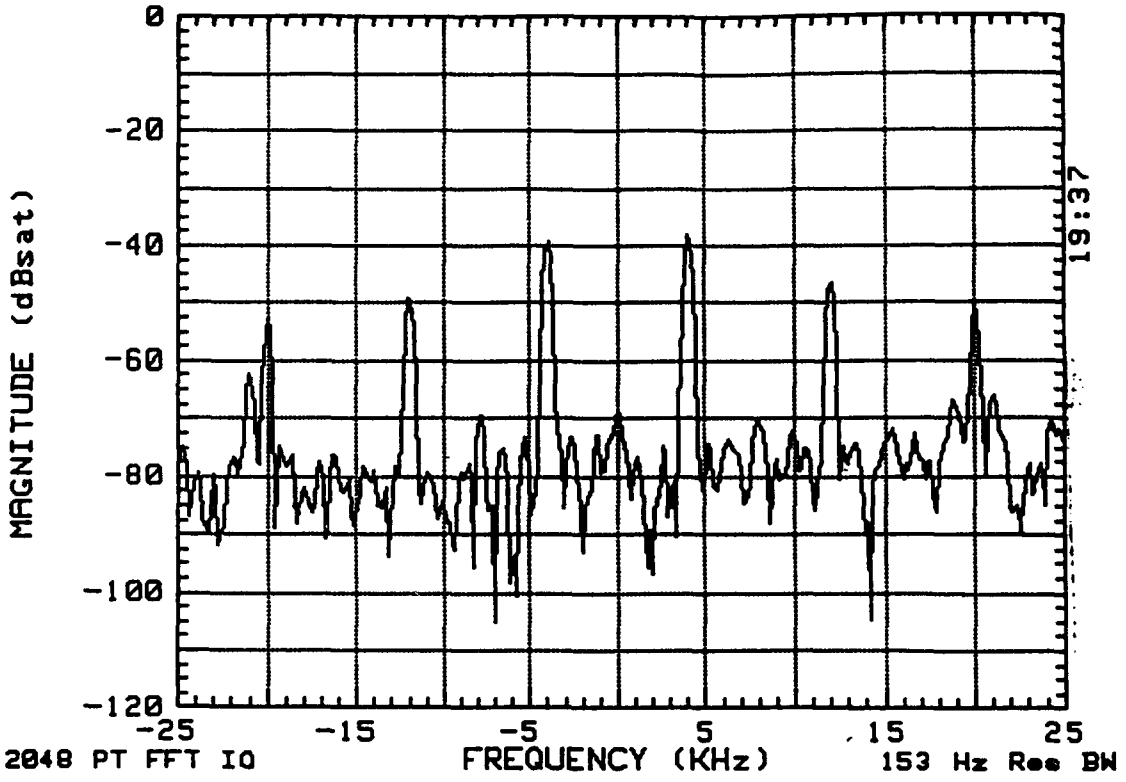

-90dBm
4kHz
BPSK

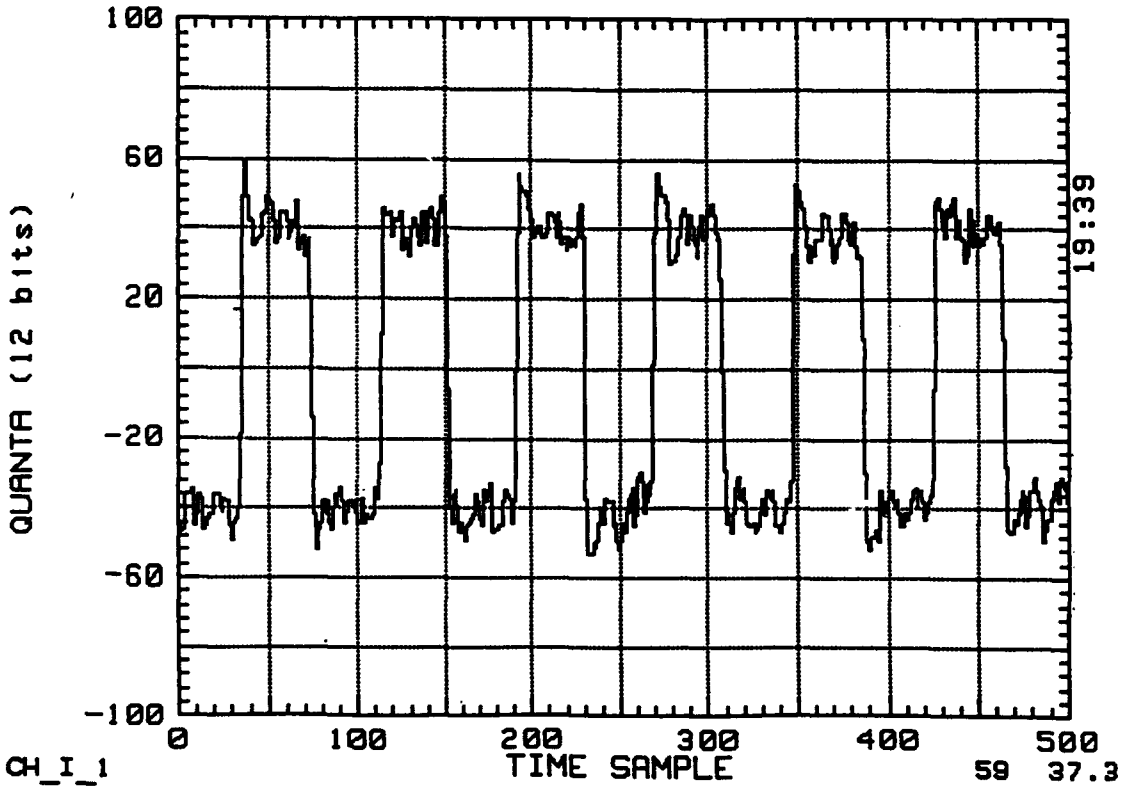

Figure 36 Various Measured Results -90dBm 4kHz BPSK

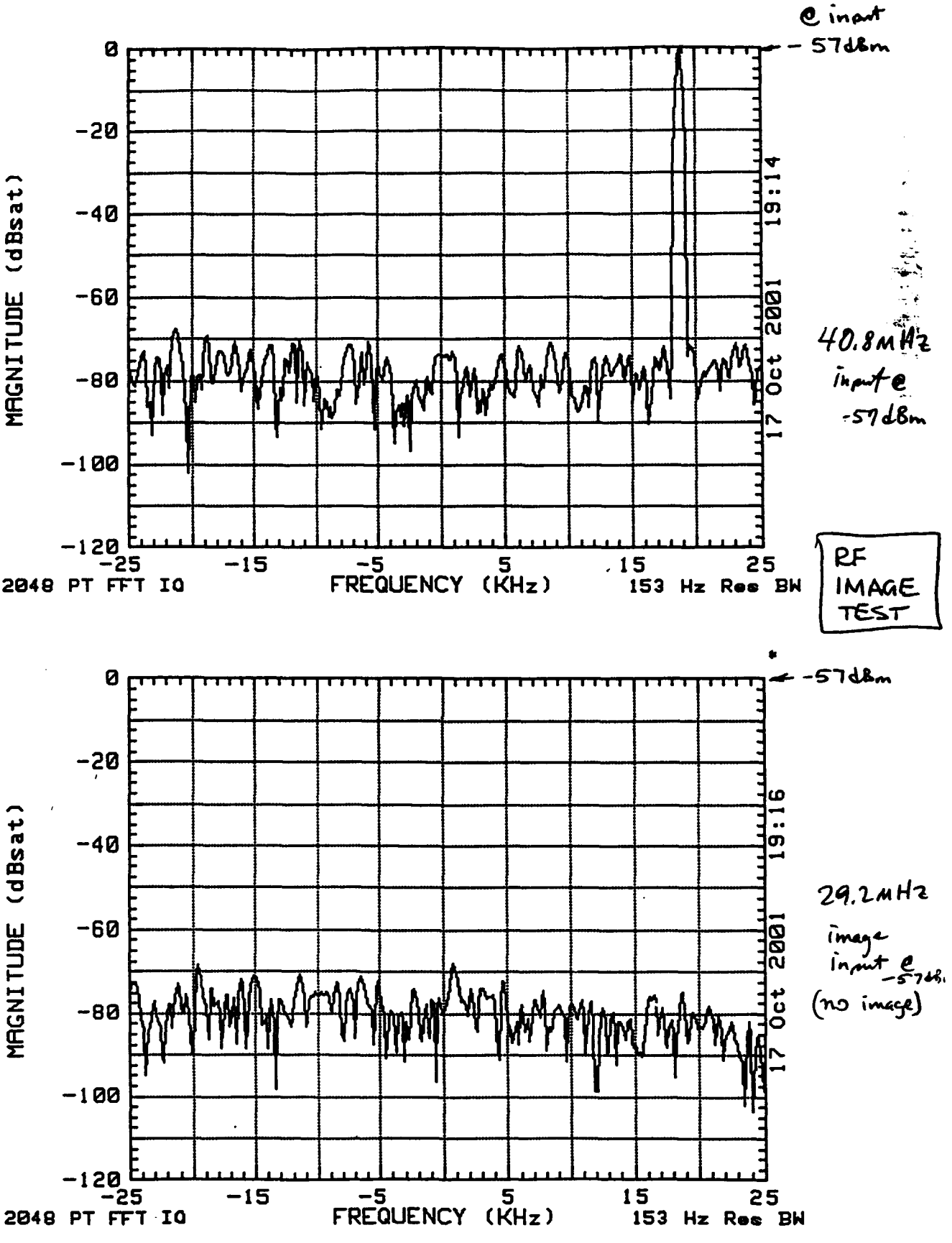

Figure 37 Various Measured Results RF Image Test

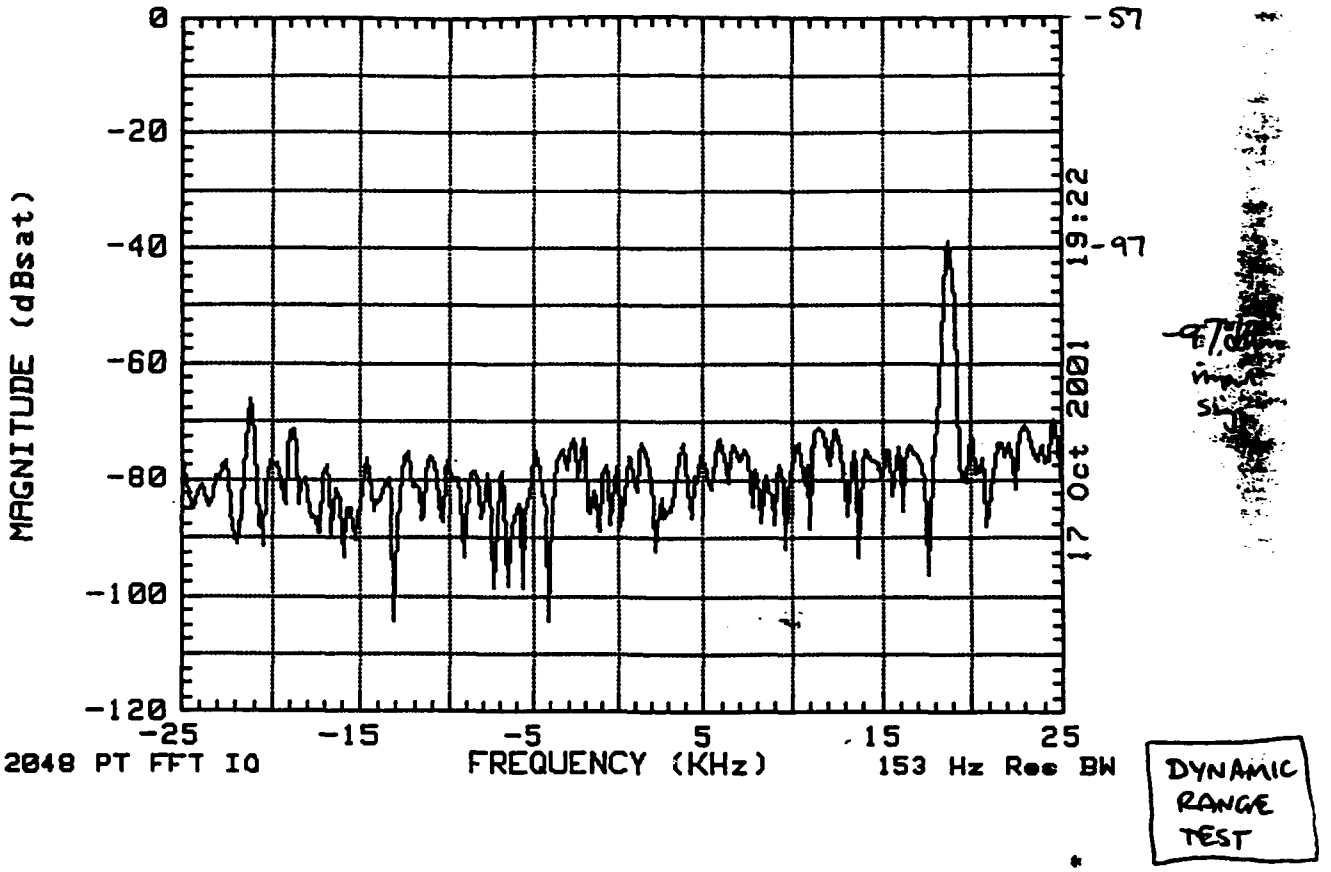

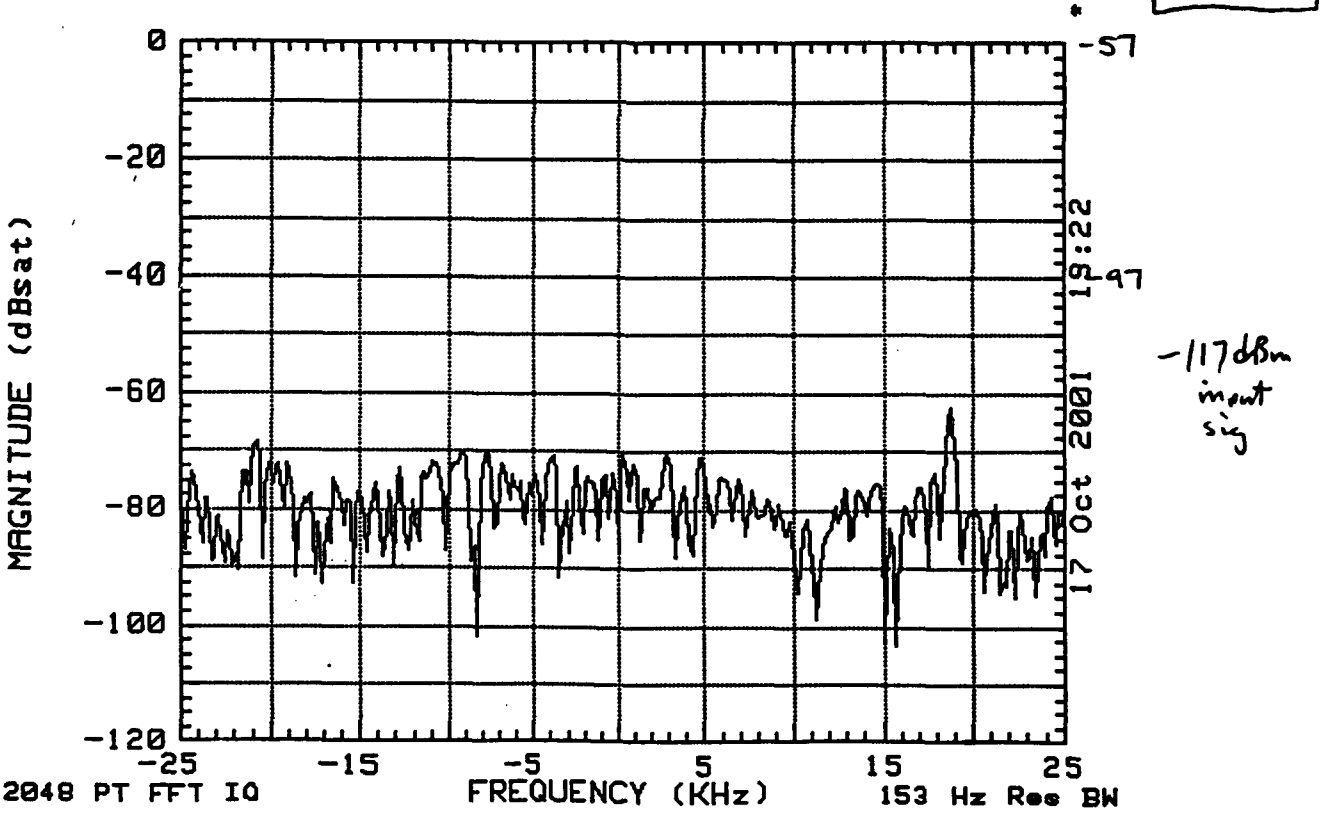

Figure 38 Various Measured Results Dynamic Range Test

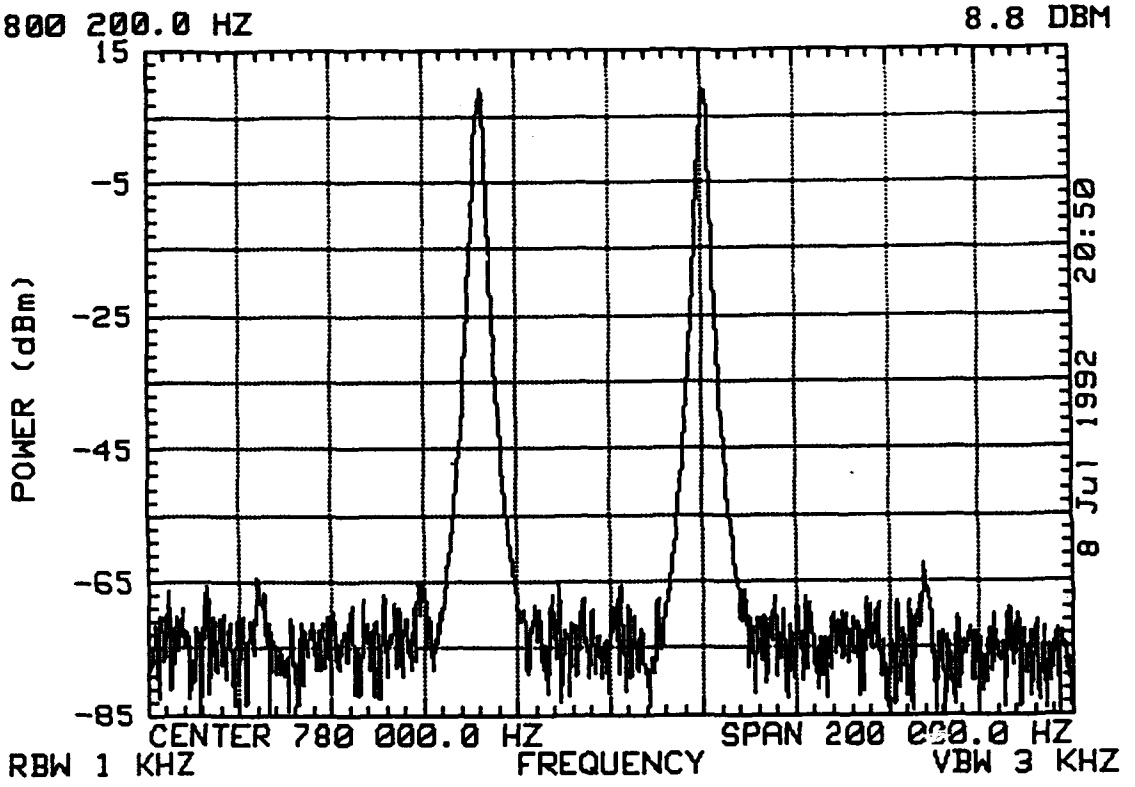

TWO TONE INTERMOD TEST

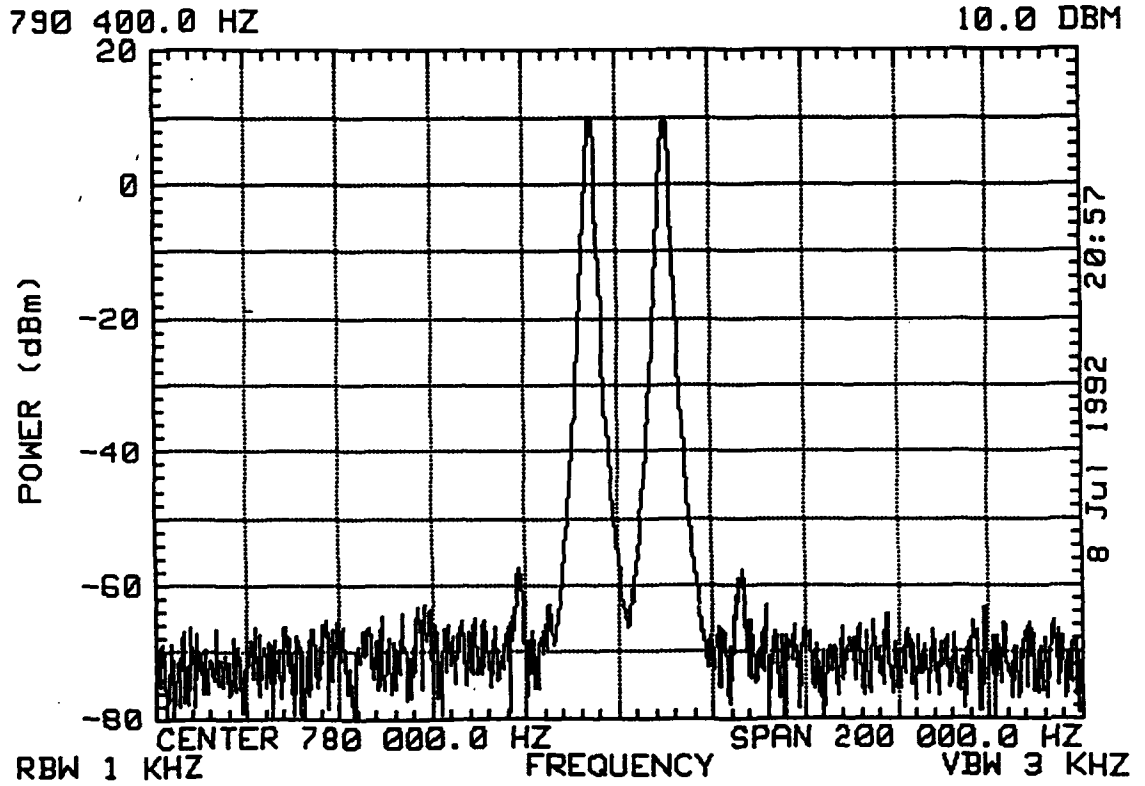

Figure 39 Various Measured Results Two Tone Intermod Test

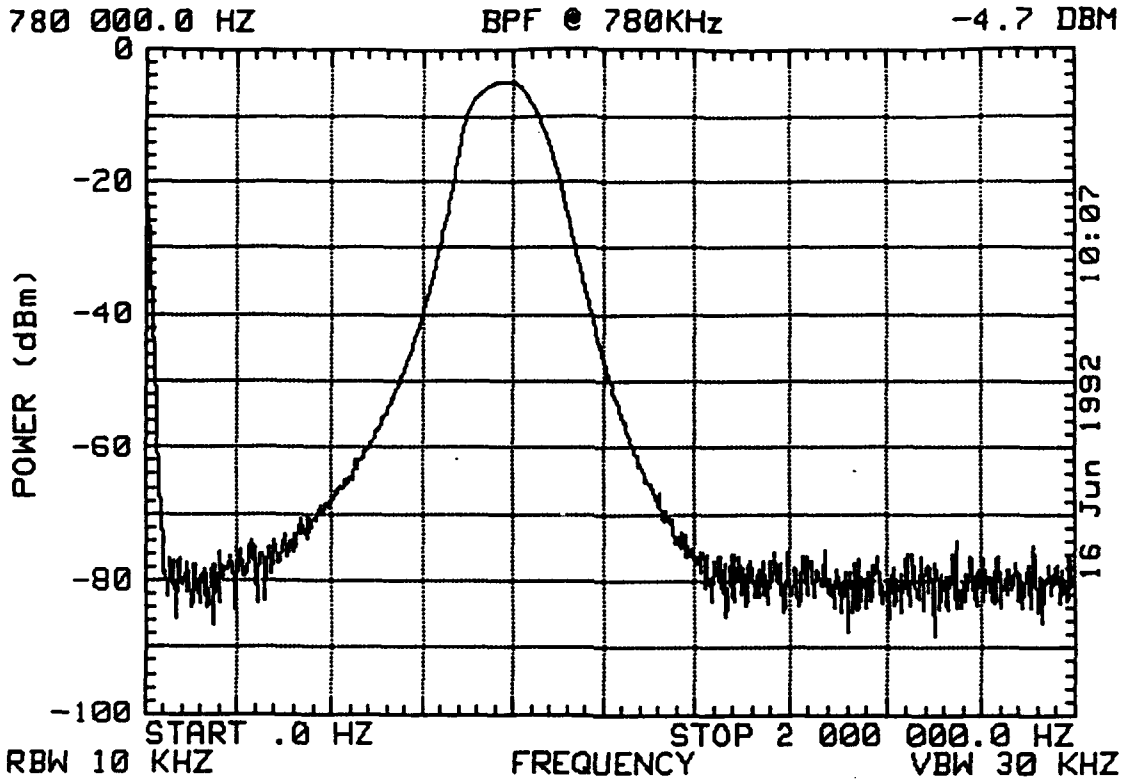

IF FILTER SHAPES

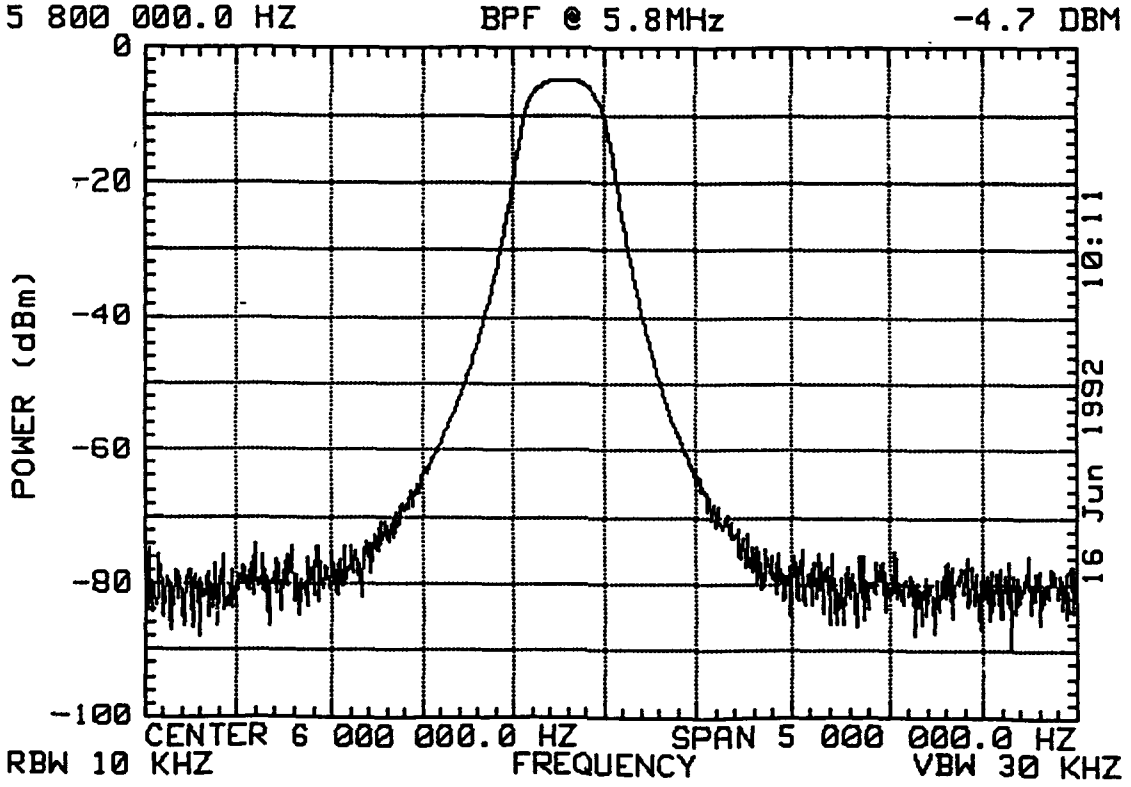

Figure 40 Various Measured Results IF Filter Shapes

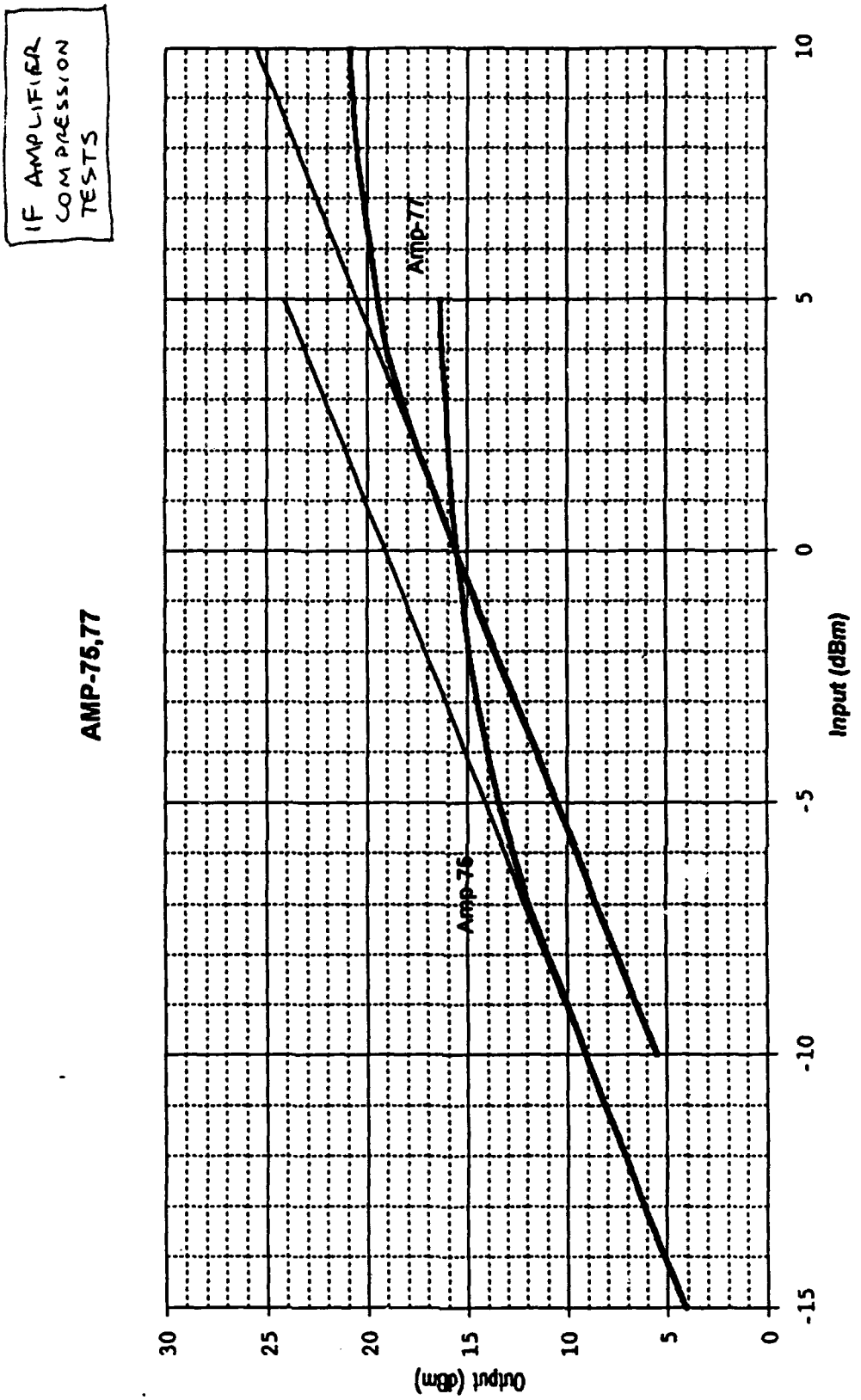

Figure 41 IF Amplifier compression Test

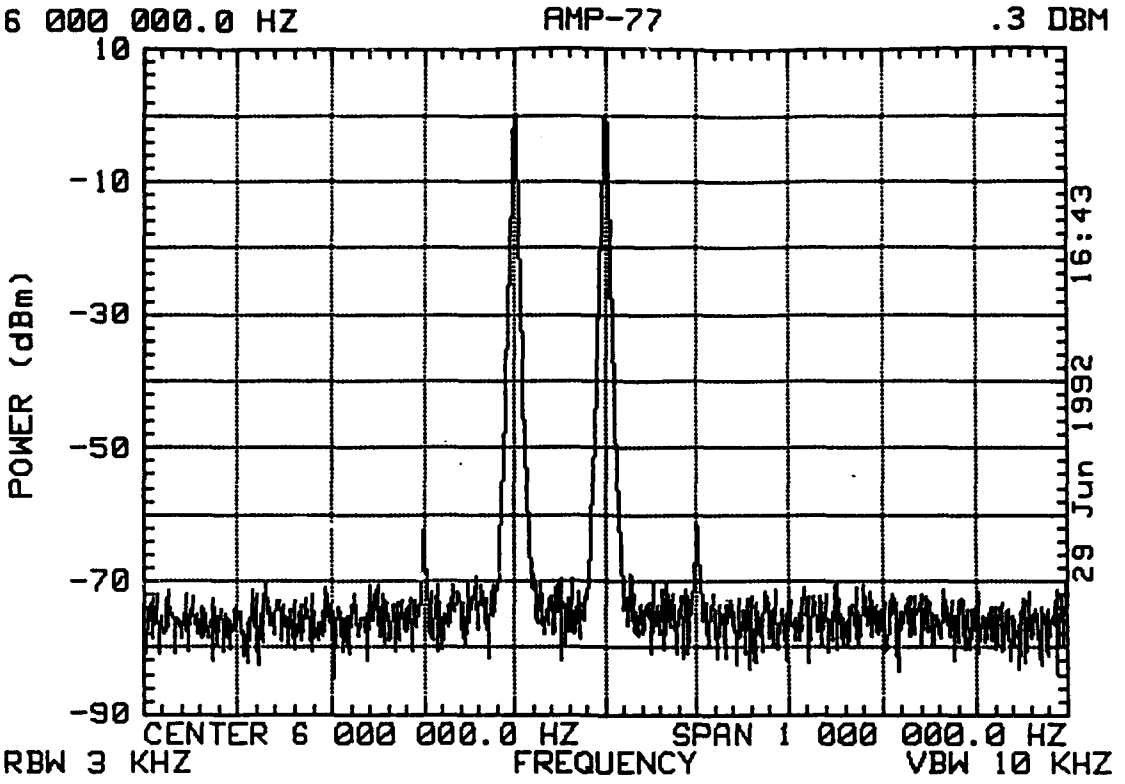

IF AMP TWO TONE TEST

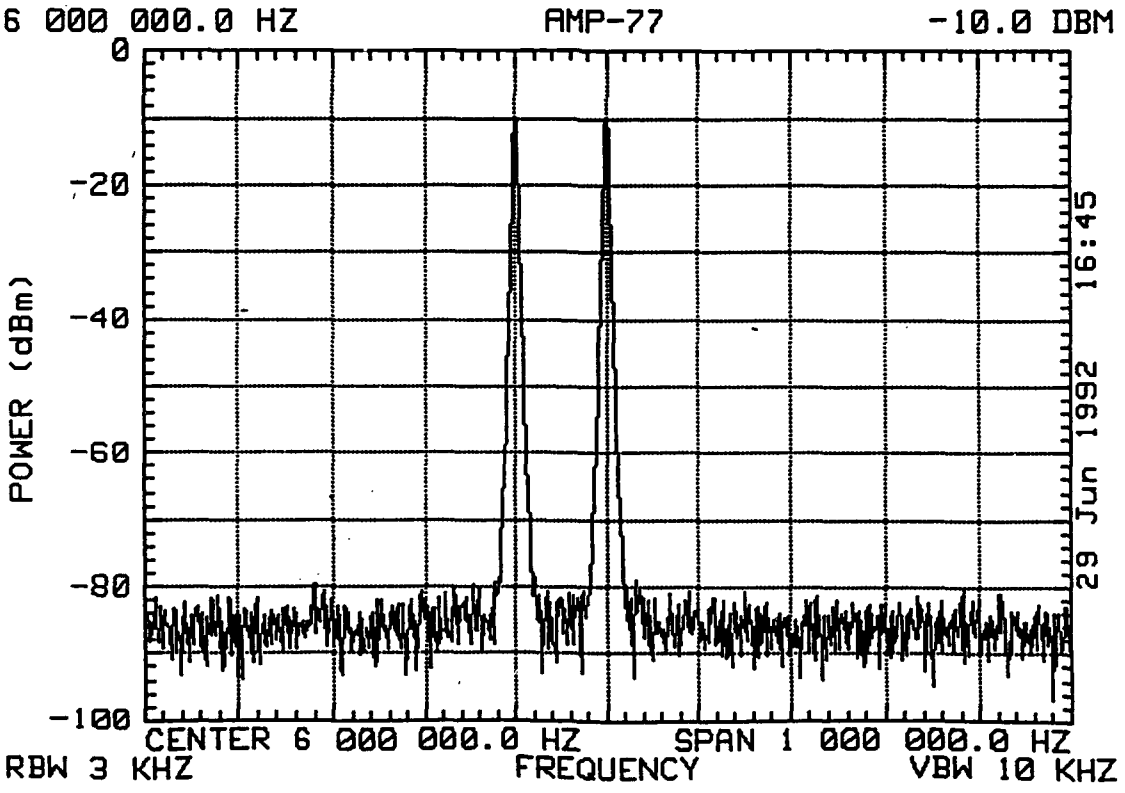

Figure 42 IF AMP Two Tone Test

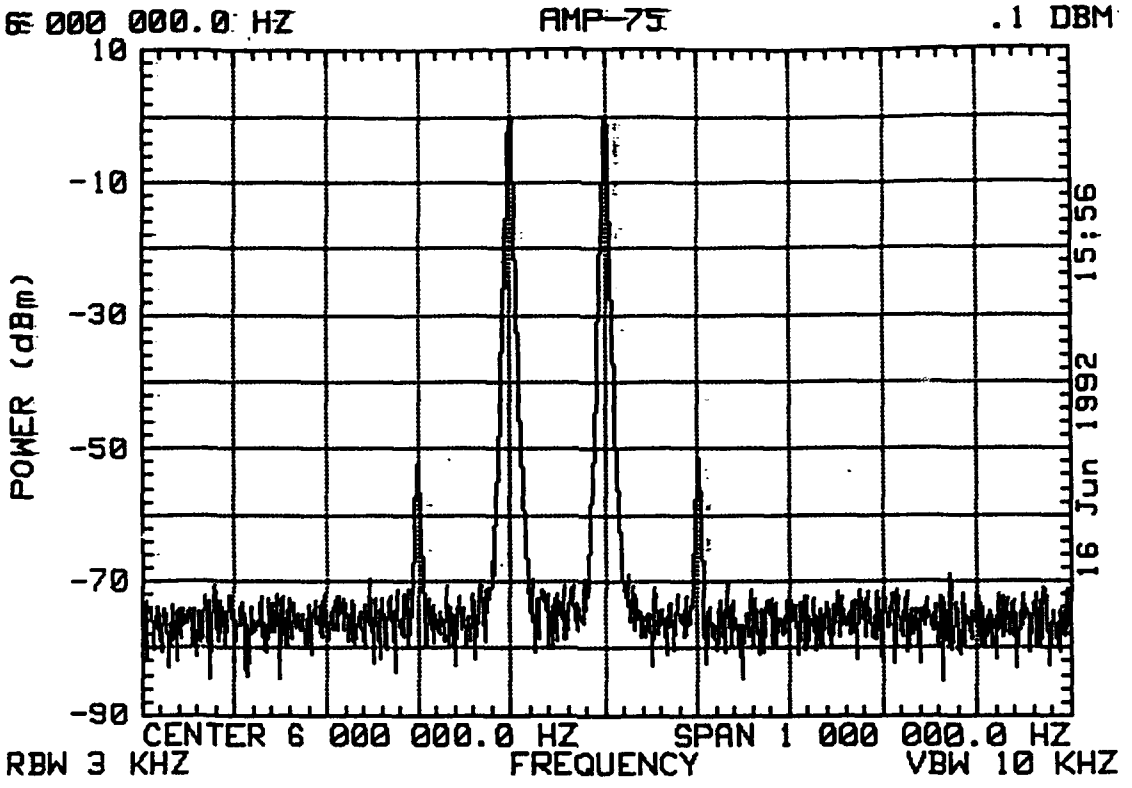

IF Amp Two Tone Test

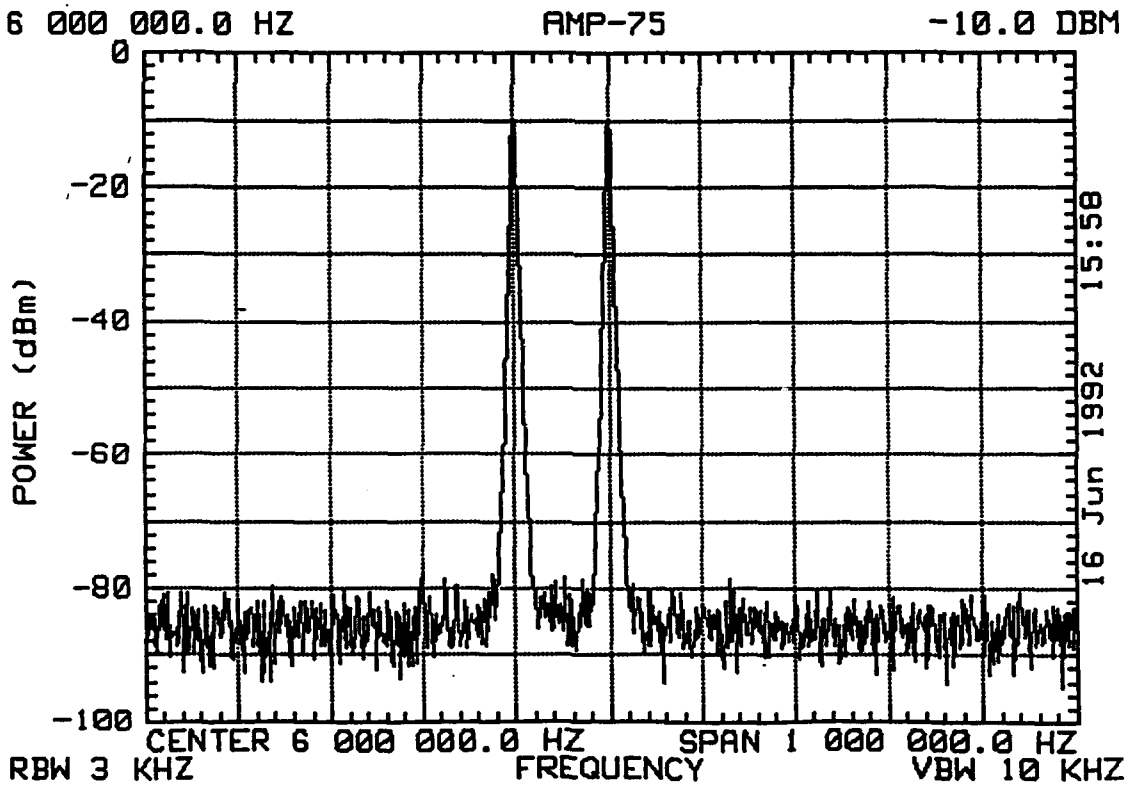

Figure 43 IF Amp Two Tone Test (Continued)